Spatial zoning of microbial functions and plant-soil nitrogen dynamics across a riparian area in an extensively grazed livestock system

Laura L. de Sosa[a,*], Helen C. Glanville[a,b], Miles R. Marshall[c], A. Prysor Williams[a], Maïder Abadie[d], Ian M. Clark[d], Aimeric Blaud[d], Davey L. Jones[a]

[a] *School of Environment, Natural Resources & Geography, Bangor University, Deiniol Road, Bangor, Gwynedd, LL57 2UW, United Kingdom*

[b] *School of Geography, Geology and the Environment, Keele University, Keele, Staffordshire, ST5 5BG, United Kingdom*

[c] *Centre for Ecology and Hydrology, Environment Centre Wales, Deiniol Rd, Bangor, Gwynedd, LL57 2UW, United Kingdom*

[d] *Department of Sustainable Agriculture Sciences, Rothamsted Research, West Common, Harpenden, Hertfordshire, AL5 2JQ, United Kingdom*

* Corresponding author. School of Environment, Natural Resources & Geography, Bangor University, Deiniol Road, Bangor, Gwynedd, LL57 2UW, United Kingdom.

E-mail address: afs411@bangor.ac.uk (L.L. de Sosa).

ABSTRACT

Anthropogenic activities have significantly altered global biogeochemical nitrogen (N) cycling leading to major environmental problems such as freshwater eutrophication, biodiversity loss and enhanced greenhouse gas emissions. The soils in the riparian interface between terrestrial and aquatic ecosystems may prevent excess N from entering freshwaters (e.g. via plant uptake, microbial transformations and denitrification). Although these processes are well documented in intensively managed agroecosystems, our understanding of riparian N removal in semi-natural systems remains poor. Our aim was to assess the spatial zoning of soil microbial communities (PLFA), N cycling gene abundance (archaeal and bacterial *amoA*, *nifH*, *nirK*, *nirS*, *nosZ*), N processing rates and plant N uptake across an extensively sheep grazed riparian area. As expected, soil properties differed greatly across the riparian transect, with significant decreases in organic matter, NH_4^+, carbon (C) and N content closest to the river (< 10 m). In addition, different microbial community structures were found along the transect. The abundance of N fixation (*nifH*) increased with distance from the river (> 10 m), while ammonia oxidising archaea (AOA) increased in abundance towards the river. N_2O emissions rates were limited by C and to a lesser extent by N with greater emissions close to the river. Plant uptake of urea-derived ^{15}N was high (ca. 55-70% of that added to the soil) but 30-65% of the N was potentially lost by denitrification or leaching. Percentage recovered also suggests that the spatial patterning of plant and microbial N removal processes are different across the riparian zone. Our study provides novel insights into the underlying mechanisms controlling the spatial variability of N cycling in semi-natural riparian ecosystems.

Keywords: buffer strip, ecosystem services, DON, nitrification, heathland, wetlands.

1. Introduction

The overuse of nitrogen (N) fertilizers, alongside land use change, has caused the N saturation of many terrestrial ecosystems worldwide (Gruber and Galloway, 2008). Further, the resultant N loss from agroecosystems is contributing to many major environmental problems such as marine and freshwater eutrophication, loss of biodiversity, climate change and ecosystem acidification (Canfield et al., 2010; Erisman, 2013). Strategies are therefore needed to better retain, or sustainably remove, excess N from land under agricultural production. One potential mechanism is the active management of riparian areas at field margins to intercept and mitigate excess N from migrating towards freshwaters (Mayer et al., 2007). Within these areas, a range of interrelated biotic and abiotic processes may be involved in N attenuation, including nitrification, denitrification, mineralization, plant and microbial uptake, mass flow/diffusion and sorption-desorption (Matheson et al., 2002; Vyzamal, 2007). The importance of each process, however, is expected to vary greatly between ecosystems and also from the landscape down to the micrometre scale within the plant-microbial-soil system (Burt et al., 1999; Sanchez-Pérez et al., 2003).

Denitrification has been shown to be of particular importance for riparian wetland biogeochemistry because of the predominance of anoxic conditions, high concentrations of dissolved organic carbon (DOC) and the high rates of N fixation (Groffman and Hanson, 1997). It also represents the ultimate removal mechanism for reactive nitrogen (e.g. NO_3^-, NO_2^-, N_2O) from terrestrial and aquatic ecosystems (Seitzinger et al., 2006; Jacinthe and Vidon, 2017). In some cases, however, complete denitrification to N_2 may not occur due to a lack of N_2O reductase in the microbial community or if certain environmental conditions remain sub-optimal (e.g. soil moisture, O_2 content), leading to the potential release of environmentally damaging N_2O

(Butterbach-Bahl et al., 2013). Additionally, denitrification is strongly coupled, both spatially and temporally, with other environmental processes such as N fixation, nitrification and anaerobic ammonium oxidation (anammox) (Vyzamal, 2007; Groffman et al., 2009).

To optimise N removal by riparian areas and to implement active management, requires a good understanding of the key factors which regulate N cycling across these zones. Fundamental to this, is understanding the spatial abundance and behaviour of the underlying microbial communities which control how and when the different N transformations occur (Herbert, 1999; Chon et al., 2011). In this respect, few studies have tried to combine the analysis of key N cycling genes (abundance and transcription) and quantification of N_2O:N_2 production to gain a better insight into the spatio-temporal factors regulating N_2O fluxes (Avrahamia and Bohannan, 2009)). However, contradictory studies showing a clear relationship between gene copy number and N_2O emission rates or a total lack of it, are commonly presented, highlighting the need for further research in this area (Bakken et al., 2012; Di et al., 2014). Additionally, research in wetland biogeochemistry has frequently focused on single-ecosystem processes (i.e. denitrification) rather than providing a more holistic view of microbial community functioning (Gutknech et al., 2006). Therefore, there is a need to improve our understanding of the links (from genes to ecosystems) between physical, biogeochemical and ecological processes that drive the services of freshwater systems

Alongside the microbial community, wetland vegetation also plays a major role in regulating N losses via denitrification (Schnabel et al., 1996; Veraart et al., 2011). For example, plants can alter the size and composition of the soil microbial community, stimulate microbial activity via C rhizodeposition, and change soil oxidation status (Nijburg et al., 1997; Tabuchi et al., 2004; Groffman et al., 2009). In addition, wetland

plants employ numerous physiological adaptations to overcome anoxia in waterlogged soils including: shallow rooting, dumping of respiratory by-products into the rhizosphere (e.g. lactic acid) and the formation of aerenchyma (Wheeler, 1999). In light of this, the choice of plant species is likely to be very important for improved riparian management and freshwater protection.

While much work has been undertaken on N removal in riparian areas adjacent to intensive cropping systems, comparatively little work has been undertaken in extensively grazed livestock systems (Wells et al., 2016). In these systems, urine hotspots represent the major input of reactive N and are expected to greatly modify soil microbial communities involved in N cycling (Di et al., 2010). In this context, the main objectives of the present study were: (1) to gain further insight into the environmental factors controlling riparian soil N cycling and how they contribute to explaining the spatial and temporal variability of N cycling in semi-natural ecosystems; (2) to estimate the role of different vegetation communities in N uptake across the riparian zone; and (3) to link N cycling gene abundance to N removal processes.

2. Materials and methods

2.1. Study site

The experimental site was located in the upper, southern area of the Conwy catchment, North Wales, UK (52° 59' 8.90"N, 3° 49' 15.99"W; Fig. 1; Figs. S1 and S2). The study area has been classified as blanket bog according to the New Phase 1 habitat survey (Lucas et al., 2011) and considered a Special Area of Conservation (SAC) under the EC Habitats Directive (94/93/EEC). The climate of the upper reaches of the Conwy catchment is characterized by relatively high rainfall and cool temperatures (mean annual rainfall of 2180 mm and mean annual soil temperature at 30 cm depth is 8 °C;

based on 30-year average 1981-2010 data from the UK Met Office). The area was subject to sheep (*Ovis aries* L.) grazing at a low stocking density (0.1 ewe ha^{-1}). A detailed description of the Conwy catchment and land use can be found in Emmett et al. (2016) and Sharps et al. (2017).

2.2. Sampling strategy

Four 25 m long transects, 5-10 m apart, and perpendicular to a headwater stream of the Conwy River, were delineated for sampling during the month of October 2016 (Fig. 2). The maximum length of the transects was decided according to the extent of the riparian zone as defined by the variable buffer delineation method (de Sosa et al., 2017). Intact soil cores (5 cm diameter, 0-15 cm depth) were collected at three different zones (from this point onwards in the manuscript, these are referred to as zones 1, 2 and 3), selected according to their dominant vegetation cover (Fig. 2). Zone 1 was dominated by thick tufts of soft rush (*Juncus effusus* L.) and located < 5 m to the river. Zone 2 corresponded to the transitional area between the grasses and the heathland (5-10 m) and zone 3 (> 10 m) represented the area dominated by typical peat-forming heathland species such as bog-mosses (*Sphagnum* spp.), *Calluna vulgaris* (L.) Hull, *Erica tetralix* L. and *Scirpus cespitosus* L. (Fig. S1-S2). Along each transect, two sample points were located within zone 1 (2 and 5 m from the edge of the river), one sample point was located within zone 2 (5-10 m), and two sampling points were located in zone 3 (i.e. 15 and 25 m; Fig. 2).

Intact soil cores were taken with a Russian auger (5 cm diameter, 15 cm in length; Eijkelkamp Soil & Water, Giesbeek, The Netherlands) to conduct the main denitrification experiment. Additional intact soil cores were taken for analysis of soil physicochemical properties prior to conducting the laboratory study and a further 20

cores for bulk density determination. All soil samples were stored at 4 °C prior to analysis except for subsamples (~25 g) which were used for Phospholipid Fatty Acid analysis (PLFA) and DNA extractions. These samples were stored immediately at -80 °C.

2.3. General soil characterization

Soil samples were passed through a 2 mm sieve to remove any plant material and to ensure sample homogeneity. They were held at field moisture for all subsequent analyses to represent field conditions. Soil water content was determined gravimetrically (24 h, 105 °C) and soil organic matter content was determined by loss-on-ignition (LOI) (450 °C, 16 h). Soil pH and electrical conductivity (EC) were measured using standard electrodes in a 1:2.5 (*w*/*v*) soil-to-deionised water mixture. Total available ammonium (NH_4-N) and nitrate (NO_3-N) in soil were determined within 0.5 M K_2SO_4 extracts (1:5 *w*/*v*) via the colorimetric salicylate procedure of Mulvaney (1996) and the vanadate method of Miranda et al. (2001), respectively. Available phosphate (P) was quantified with 0.5 M acetic acid extracts (1:5 *w*/*v*) following the ascorbic acid-molybdate blue method of Murphy and Riley (1962) and total C (TC) and N (TN) were determined with a TruSpec® elemental analyser (Leco Corp., St Joseph, MI). Dissolved organic C (DOC) and total dissolved N (TDN) were quantified in 1:5 (*w*/*v*) soil-to-0.5 M K_2SO_4 extracts (Jones and Willett, 2006) using a Multi N/C 2100 TOC analyzer (AnalytikJena, Jena, Germany). Total soil porosity was determined using the equation of 1-(bulk density/particle density for organic soils) and percent water-filled pore space (WFPS) was obtained from the relationship between the volumetric water content and total soil porosity. Anaerobic mineralizable N (AMN) was determined by the anaerobic incubation of soil samples for 14 days at 25-30 °C in the

dark, followed by extraction with 1 M KCl and measurement of NH_4-N produced as described above (Bundy and Meisinger, 1994). Anaerobically mineralizable organic C (AMOC) was calculated as described in Ullah and Faulkner (2006). Briefly, moist soil samples were placed in gas-tight containers and NO_3^- was added to remove any soil limitation. Containers were purged with N_2 gas to induce anoxic conditions and stored in the dark at room temperature (25 ºC). The headspace of the containers was sampled after 1, 24, 48 and 72 h of incubation and analysed for CO_2 concentration on a Clarus 500 gas chromatograph with a TurboMatrix headspace autoanalyzer (Perkin-Elmer Inc., Waltham, CT).

2.4. Phospholipid fatty acid analysis

Microbial community structure was measured by phospholipid fatty acid (PLFA) analysis following the method of Buyer and Sasser (2012). Briefly, samples (2 g) were freeze-dried and Bligh-Dyer extractant (4.0 ml) containing an internal standard added. Tubes were sonicated in an ultrasonic bath for 10 min at room temperature before rotating end-over-end for 2 h. After centrifuging (10 min) the liquid phase was transferred to clean 13 mm × 100 mm screw-cap test tubes and 1.0 ml each of chloroform and water added. The upper phase was removed by aspiration and discarded while the lower phase, containing the extracted lipids, was evaporated at 30 °C. Lipid classes were separated by solid phase extraction (SPE) using a 96-well SPE plate containing 50 mg of silica per well (Phenomenex, Torrance, CA). Phospholipids were eluted with 0.5 ml of 5:5:1 methanol:chloroform:H_2O (Findlay, 2004) into glass vials, the solution evaporated (70 °C, 30 min). Transesterification reagent (0.2 ml) was added to each vial, sealed and incubated (37 °C, 15 min). Acetic acid (0.075 M) and chloroform (0.4 ml each) were then added. The chloroform was evaporated just to

193 dryness and the samples dissolved in hexane. The samples were analysed with a 6890
194 gas chromatograph (Agilent Technologies, Wilmington, DE) equipped with
195 autosampler, split-splitless inlet, and flame ionization detector. Fatty acid methyl esters
196 were separated on an Agilent Ultra 2 column, 25 m long × 0.2 mm internal diameter ×
197 0.33 µm film thickness. Standard nomenclature was followed for fatty acids (Frostegård
198 et al., 1993). A detailed description of PLFA markers and taxonomic microbial groups
199 is provided in Table S1.
200
201 *2.5. Denitrification and potential N_2O emissions*
202 Denitrification rates were measured using the acetylene (C_2H_2) block method
203 based on the intact core technique developed by Tiedje et al. (1989). Although this
204 technique presents limitations such as the poor diffusion of C_2H_2 into the soil, it has
205 been found to produce similar results to experiments using ^{15}N tracers (Aulakh et al.,
206 1991).
207 In brief, intact soil cores (approximately 37 ± 1.5 g dry weight soil) were placed in
208 PVC tubes (10 × 15 cm) to maintain soil structure. These tubes were then placed in gas-
209 tight containers (1.4 dm^3 volume; Lock & Lock Ltd., Seoul, Republic of South Korea).
210 To measure denitrification, 20 ml of 4 different C and N amendments were
211 applied to individual soil cores (n = 20 per amendment):
212 1) Control (distilled water addition only)
213 2) Glucose-C addition (glucose solution containing 4 g C l^{-1}; 55 mM glucose)
214 3) Urea-N addition (artificial sheep urine containing 2 g N l^{-1}; Selbie et al., 2015)
215 4) Urea-N + glucose-C addition (artificial urine plus glucose solution containing 2
216 g N l^{-1} and 4 g C l^{-1} respectively).

Urea was selected as it represents one of the main N inputs to upland grazed ecosystems. The N concentration was chosen according to the concentration range in urine under a light grazing regime (Selbie et al., 2015). The ratio of C-to-N was chosen based on experimental values presented in Her and Huang (1995). Glucose was chosen as it represents a labile C substrate that can be utilized by almost all soil microorganisms (Gunina and Kuzyakov, 2015). The concentration of added C also reflects a typical sugar concentration that would occur in soil upon root cell lysis (Jones and Darrah, 1996).

All cores were directly injected with 5 ml of C_2H_2 into the middle of the soil volume. The cores were then placed into gas-tight containers and 10% of the headspace replaced with C_2H_2 to block the conversion of N_2O to N_2 gas. The control cores were only amended with 20 ml of distilled water without C_2H_2 addition. The containers were stored at 10 ºC in the dark to prevent C_2H_2 breakdown. Headspace gas was sampled at 0, 2, 6 and 24 h and stored in pre-evacuated 20 ml glass vials before being analysed for N_2O concentration on a Clarus 500 gas chromatograph with a TurboMatrix headspace autoanalyzer (Perkin-Elmer Inc., Waltham, CT). Prior to gas sampling, the headspace was homogenised by gently mixing with a syringe. At the end of the experiment, each individual core was weighed and N_2O fluxes corrected accordingly. The rate of N_2O production was calculated in μg $N\text{-}N_2O$ g^{-1} dw h^{-1}. Cumulative N_2O emissions were calculated by integration using the trapezoidal rule.

2.6. Nitrogen uptake by vegetation

The role of vegetation in N uptake was measured in the field using ^{15}N-labelled urine. Two independent sets of plots (50 cm times 50 cm) were randomly selected

within each replicate vegetation zone, one set received no N additions (herein referred to as the control set) while the second received ^{15}N-labelled artificial urine.

Prior to addition of the ^{15}N-labelled treatment, turfs (20 cm times 20 cm) and associated soil (0-15 cm depth) were taken from the centre of each of the control plots to obtain ^{15}N natural abundances for each plant and soil component. After harvest, the samples were transferred to the laboratory and separated into soil, roots, shoots and mosses for ^{15}N determination. Subsequently, in each ^{15}N-labelling plot, 250 ml of artificial urine labelled with ^{15}N urea (15 atom %) at a rate of 2 g N l^{-1} was applied (equivalent to 20 kg N ha^{-1}). Ten pulses of ^{15}N-labelled urine (each pulse was 25 ml in volume) were injected with a syringe (0.84 mm bore × 5 cm long) into the soil underneath the plants (0-15 cm depth) in the centre of the plot. Depth of urine injection was selected according to previous observations of urine infiltration into the soil. The volume and concentration of N added followed that of a typical sheep urine event (Marsden et al., 2016). Immediately after the final ^{15}N pulse addition, the area was protected with individual wire mesh cages to prevent livestock trampling and grazing. One week after ^{15}N addition, a 20 × 20 cm^2 turf and associated soil (0-15 cm depth) was harvested from the middle of each plot, transferred to the laboratory and separated into soil and plant components as described above for ^{15}N determination.

Soil for ^{15}N analysis was passed through a 2-mm sieve and subsamples (ca. 40 g) were oven-dried (48 h, 80 °C) before being weighed and ground for ^{15}N analysis. Plant shoot and root material followed the same drying procedure after being washed with distilled water to remove any exogenous isotope label. The same procedures were followed for the control samples one week before to avoid any cross-contamination with the ^{15}N-urea labelled samples. All fractions were analysed separately for δ^{15}N at the UC Davis Stable Isotope Facility (UC Davis, Davis, CA). Values of ^{15}N are

266 presented directly as the atom% of ^{15}N in the sample. The ^{15}N atom% excess was
267 calculated as the ^{15}N atom% difference between enriched samples and values of
268 background natural abundances (control). Recovery of tracer ^{15}N (%) was calculated by
269 multiplying the N content in the pool by it mass per square meter and ^{15}N atom% excess
270 divided by total added ^{15}N per square meter (Xu et al., 2011).
271
272 *2.7. DNA extraction and quantitative PCR*
273 A subsample of soil (ca. 25 g) was taken from each of the cores used for
274 physicochemical analysis and stored at -80 °C prior to DNA extraction. The DNA was
275 extracted from three 250 mg subsamples using an UltraClean® Microbial DNA Isolation
276 Kit (Mo Bio Laboratories Inc., Carlsbad, CA) following the manufacturer's instructions.
277 Triplicate DNA extractions for each soil sample were pooled together to give a total
278 volume of 150 µl. Extractions of DNA were concentrated to give a final volume of 50
279 µl using a Savant SVC100H SpeedVac Concentrator (ThermoFisher Scientific Inc.,
280 Waltham, MA). Extracted DNA was visualized by 0.9% agarose gel electrophoresis and
281 nucleic acid staining with SafeView® (NBS Biologicals, Huntingdon, UK). The
282 concentrations of DNA where checked using Quant-iT™ dsDNA Assay Kit
283 (ThermoFisher). Samples were then stored at -80 °C prior to further analysis.
284 Microbial N cycling gene abundance was investigated by quantitative-PCR
285 (qPCR) targeting specific genes or genetic regions. Bacterial and archaeal communities
286 were targeted via the 16S rRNA genes, while the fungal community abundance by the
287 ITS region. The different communities involved in N-cycling were investigated: N
288 fixation (*nifH* gene); nitrification by targeting the ammonia oxidising bacteria (AOB)
289 and archaea (AOA) (*amoA* gene), and denitrifiers via the nitrite reductase (*nirK* and *nirS*
290 genes) and the nitrous oxide reductase (*nosZ* genes clade I and II) (Table S2).

Quantitative-PCR amplifications were performed in 10 µl volumes containing 5 µl of QuantiFast (Qiagen, Manchester, UK), 2.8 µl of nuclease-free water (Severn Biotech, Kidderminster, UK), 0.1 µl of each primer (1 µM) and 2 µl of template DNA at 5 ng μl^{-1}, using a CFX384 Touch® Real-Time PCR Detection System (Bio-Rad, Hemel Hempstead, UK). The standards for each molecular target were obtained using a 10-fold serial dilution of PCR products amplified from an environmental reference DNA (also used as positive control) and purified by gel extraction using the Wizard® SV Gel and PCR Clean Up System (Promega, Southampton, UK) following the manufacturer's instruction and quantified by fluorometer Qubit® 2.0 dsDNA BR Assay Kit (Thermo Fisher Scientific). Standard curve template DNA and the negative/positive controls were amplified in triplicate. Amplification conditions for all qPCR assays consisted in 2 steps: first denaturation at 95 °C for 5 min followed by 40 cycles at 95 °C for 10 s and 60 °C for 30 s that included annealing, elongation and reading. Each amplification was followed by melting curve (increase in temperature from 60 °C to 95 °C, with a reading every 0.5 °C) to assess the specificity of each assay. The efficiency of the qPCR varied between 81.5% and 94.5%, and r^2 between 0.996 and 0.999. The melting curves showed specificity for all the genes, except as expected for the fungal ITS, that showed the amplification of products of different lengths, due to the variability in length of the ITS region between different fungal taxa (Manter and Vivanco, 2007).

2.8. Statistical analysis

Statistical analysis was performed with SPSS v22 for Windows (IBM Corp., Armonk, NY). All data were analysed for normality and homogeneity of variance with Shapiro Wilk's tests and Levene's statistics, respectively. Transformations (log_{10} or square root) to accomplish normality and homogeneity of variance were done when

necessary (i.e. bulk density, available P, microbial biomass PLFA, ^{15}N recovery, and cumulative N_2O, untransformed values are presented). For all statistical tests, $P < 0.05$ was selected as the significance cut-off value. Analysis of variance (one-way ANOVA) was performed to explore the difference of soil physicochemical properties, gene copy numbers, PLFA ratios of microbial groups respective to distance from the river followed by Tukey's post-hoc test to assess differences across the riparian transect. Principal component analysis (PCA) was used to explore the spatial relationships of PLFA microbial groups (%) relative to distance from the river. Cumulative N_2O emissions after treatment application across the riparian transect were compared by Welch's test followed by Games-Howell post-hoc test, due to the data not conforming to homogeneity of variance even after data transformation. In contrast, a one-way ANOVA followed by Tukey's post-hoc test was performed to assess differences in cumulative N_2O emissions between treatments for each sampling distance from the river (i.e. 2, 5, 10, 15 and 25 m). Two separate analyses were conducted to explore differences in ^{15}N recovery due to the data not conforming to homogeneity of variance even after data transformation. A one-way ANOVA and Tukey's post-hoc test was performed to explore differences in the percentage allocation of ^{15}N to the different fractions (e.g. shoots, roots, moss and soil) across the different riparian zones. A second one was used to assess how ^{15}N recovery differed within each specific fraction across the three zones. A mixed model was also performed with distance from the river as a fixed effect and transect as a random effect to assess ^{15}N recovery and gene copy number across the riparian zone, but the results did not differ from ANOVA, and only the ANOVA results is presented in the article

Spearman rank correlation coefficients (ρ) were used to evaluate the relationship between soil physicochemical properties and cumulative N_2O emissions, gene copy

number, or PLFA biomarkers ratio whereas linear regressions (r^2) were used between soil physicochemical properties and PLFA biomarker ratios.

3. Results

3.1. General soil characterization

Significant differences in all soil properties, except for NO_3^- and total dissolved N concentration and anaerobic mineralizable N (AMN), were found across the riparian transect relative to distance from the main river channel (Table 1). Zone 2 showed an increase in pH values by 0.66-0.85 unit in comparison with zone 1 and zone 3. Likewise, EC was approximately 2-fold greater in zone 1 and 3 relative to zone 2. In addition, soil organic matter (SOM) tended to increase with distance from the river being 60% higher at the distal points (15 and 25 m) compared with those closer to the river. The high SOM levels associated with soils furthest away from the river contributed to lower bulk densities, higher soil porosities and increased soil water content. Available NH_4^+ concentrations were 3.6 greater in soil from zone 3 in comparison with zone 1 and 1.8 times greater than the soil in zone 2, while NO_3^- did not show any significant differences. Similarly, available P was 10-times greater in zone 3 relative to zones 1 and 2. Total C, total N and the C-to-N ratio were greater in zone 3 relative to zones 1 and 2 and a similar trend was also observed for DOC.

Anaerobic incubation of soils across the transect showed that the amount of AMOC in zone 3 was significantly greater than in zone 1 and 2 (~ 3 and 1.5 times, respectively) (Table 1). In contrast, AMN showed little trend across the transect.

3.2 Microbial community structure and abundance

Microbial biomass determined from total PLFA content showed a general decline across the riparian transect towards the river channel. Principal Component Analysis (PCA) of PLFA microbial groups (% abundance) across the transect explained 72.6% of the total variance within the dataset on the first two principal components (PC) (Fig. 3). The spatial segregation of cluster centroids within the PCA indicates that in zone 1 the most influential components were anaerobes and putative arbuscular mycorrhizal fungi (AM fungi). In contrast, Gram (+) and Gram (-) bacteria were the dominant groups in zone 2 and 3, respectively. Zone 2 showed the greatest microbial variability.

The fungi/bacteria ratio decreased by 2 to 2.5 times from zone 1 to zone 2 and 3 (Table S3, $P = 0.008$). The ratio of Gram (+)/Gram (-) was over 2 times greater in zone 2 than zone 3 but it did not differ from zone 1 ($P = 0.001$). On average, 16w/17cyclo and 18w/19cyclo ratio (indicative of an actively growing community under low stress conditions) was 2.5-fold greater in zone 3 than zone 1 and 2 (Table S3, $P < 0.0001$). There were highly positive relationships between fungi/bacteria ratio with bulk density and negatively with total porosity and soil water content ($r^2 = 0.60$, $P < 0.001$ for bulk density and total porosity, $r^2 = 0.45$, $P = 0.001$, soil water) whereas Gram (+)/Gram (-) ratio was negatively correlated to NH_4-N, soil water content, SOM, available-P and DOC content ($r^2 > 0.68$ for available P and DOC, $r^2 > 0.53$ the rest, $P < 0.001$ in all cases). In contrast, a positive correlation was found between 16w/17cyclo and 18w/19cyclo ratios and DOC, soil water, C-to-N ratio and SOM content ($r^2 > 0.61$, for DOC, $r^2 > 0.71$, for soil water and C-to-N ratio, $r^2 > 0.82$, for SOM, $P < 0.001$ in all cases).

The archaeal 16S rRNA gene abundance tended to increase with distance from the river but the results were not significantly different ($P > 0.05$) (Fig. 4). In contrast, the fungal ITS region abundance showed the opposite trend but was also not significant.

The bacterial 16S rRNA gene abundance displayed on average 2 times greater bacterial copies in zone 2 than the distal area but it was not significant (Fig. 4).

Significant positive correlations were found between bacterial *16SrRNA* and pH and EC (ρ = 0.48, -0.45, respectively) whereas archaeal *16SrRNA* correlated negatively with soil bulk density and positively with total porosity (ρ = -0.57, 0.56, respectively; Table 2).

3.2. ^{15}N uptake by the vegetation

No significant differences were found between the recovery of ^{15}N in the different plant and soil fractions across the riparian transect (zone 1, 2 and 3; $P > 0.05$). Similar percentages of total ^{15}N recovery of added ^{15}N were obtained for plants and soil in zones 2 and 3 (71.9 % and 79.3%, respectively), whereas only 56.8% was recovered in the plants and soil within zone 1 although it was not significant (Fig. 5). Generally, there were very few differences between the amounts of ^{15}N recovered in the different plant-soil fractions within each zone, Only in zone 2, were four times more ^{15}N was recovered in the shoots compared to the soil ($P = 0.012$; Fig. 5).

3.3. Potential denitrification and N_2O emissions

In response to the addition of labile C and/or N to the soil, greater cumulative N_2O emissions were only observed within zone 1, showing little or no effect in zones 2 and 3 (Fig. 6). In zone 1, the addition of labile C-only increased N_2O emissions by a factor of 1000, from 0.004 ± 0.001 to 4.07 ± 0.14 mg N kg^{-1} h^{-1} relative to the control in the area closest to the river (e.g. 2 m, $P < 0.001$). Similarly, the addition of C and N together also increased N_2O emissions relative to the control (0.004 ± 0.001 to 2.95 ± 0.14 mg N kg^{-1} h^{-1}) at 2 m from the river. After the addition of labile C alone or in

415 combination with N, emissions of N_2O were 78 and 45 times higher, respectively than
416 the control at 5 m from the river (Fig. 6). Although urea-N addition also increased N_2O
417 emissions in zone 1 (0.24 ± 0.06 mg N kg^{-1} h^{-1} at 2 m, and 0.61 ± 0.36 mg N kg^{-1} h^{-1} at 5
418 m), fluxes were not significantly different from the control ($P > 0.05$).

419 N_2O emissions across the riparian transect significantly differed for all
420 treatments with respect to the distance from the river ($P < 0.001$, treatments with C
421 addition alone or in combination with N addition; $P < 0.05$, urea-N only addition). Basal
422 emissions of N_2O from the control cores did not show significant differences with
423 distance from the river ($P > 0.05$). Carbon-only addition greatly stimulated emissions of
424 N_2O with distance from river, with the area closest to the river (2 m) emitting on
425 average 80 times more N_2O than the distal point of the transect (25 m). The addition of
426 C together with N increased N_2O emissions at 2 m from the river by 60, 90 and 101% in
427 comparison to the amount emitted at 5 m and zone 2 and 3, respectively (Fig. 6).

428 Significant positive correlations were found between N_2O emissions and bulk
429 density, whereas soil water content, total N, total porosity and AMOC correlated
430 significantly but negatively with N_2O production for all treatments except the control
431 (Table 3).

432

433 *3.4. N cycling gene abundance*

434 Ammonia oxidizing bacteria (AOB) and archaea (AOA) showed different
435 abundance patterns with respect to distance from the river (Fig. 7). While the proximity
436 of the river had no effect on the bacterial *amoA* gene numbers, archaeal *amoA* gene
437 copy number significantly decreased ($P = 0.001$) on average by up to 84% from zone 1
438 closest to the river to zone 2 and by 98% with respect to zone 3. The archaeal-to-
439 bacterial *amoA* gene ratios were approximately 5 and 46-fold greater in zone 1 relative

to zone 2 and 3 respectively (Fig. S3). In contrast, the *nifH* gene abundance significantly increased (P = 0.001) from close to the river to the distal point by 67-82%, whereas a difference with respect to zone 2 was only found for 2 m. Zone 1, specifically the closest point to the river, displayed the lowest value for *nirS* gene abundance which represents 3.5 lower values than zone 2 (P = 0.038) (Fig. 7). In contrast, *nirK* and *nosZ* gene copy numbers did not change significantly across the transect (P > 0.05). The clade II of the *nosZ* gene could not be amplified despite the positive control being amplified (data not shown)

Abundance of *nirS* and *nosZ* genes correlated positively with pH (ρ ~0.5) but negatively with EC (ρ = -0.52, -0.63, respectively) (Table 2). A negative correlation was found between *nifH* and soil bulk density while archaeal *amoA* was correlated positively with bulk density (Table 2). Significant positive correlations were found between *nifH* and soil water content, AMOC, total porosity, NH_4^+ content and microbial PLFA whereas archaeal *amoA* abundance correlated negatively to the same soil properties (Table 2). The bacterial *amoA* and *nirS* genes did not show any significant correlations.

A positive strong correlation was found between copies of bacterial *16SrRNA*, bacterial *amoA* and *nirK* (ρ > 0.73, P < 0.001 in all cases) whereas *nifH* showed a highly positive correlation with *nirK* (ρ > 0.52, P = 0.001).

4. Discussion

4.1. Soil biology and biogeochemistry across the riparian zone

The riparian zone showed distinct spatial patterns in soil properties, despite the relatively short length of the transect. Results from this study clearly showed that vegetation, influenced in turn by the prevailing hydrodynamic conditions, had a striking effect on most of the soil's physicochemical properties. This finding is supported by a

range of studies which have established that mean high water level together with the frequency of water fluctuation is a critical factor controlling species diversity and abundance close to watercourses (Wierda et al., 1997; Lou et al., 2016). In our study, there were lower amounts of soil organic matter and nutrients (N and P) in soils close to the river in comparison to those further away. These can be ascribed to differences in erosion-depositional processes occurring along the transect. Alongside differences in water table depth, this has led to the formation of two very distinct vegetation communities: one that contains species that can tolerate extreme waterlogging and anoxia (via aerenchyma formation and organic acid excretion) and high levels of exogenous Fe^{2+} and Mn^{2+} (e.g. *Juncus effusus*; Visser et al., 2006; Blossfeld et al., 2011), and another that relies on obligate aerobic symbionts, which lacks aerenchyma and can only tolerate mild hypoxia (e.g. *Calluna* heathland; Gerdol et al., 2004; Rydin and Jeglum, 2013). These differences in plants are likely to be a key driver in shaping rhizosphere microbial communities and the dominant N cycling pathways.

The microbial community structure was different in the three riparian zones due the distinct soil physicochemical properties, and plant cover that are highly dependent on local hydrological regime (Gutknecht et al., 2006; Balasooriya et al., 2007). For example, the fungal-to-bacterial ratio was very low indicating a clear dominance of bacteria community over fungi. Nevertheless, the higher ratios in areas close to the river suggests a zonation pattern in fungal communities across the transect, probably linked to plant type and poor nutrient conditions (Bohrer et al., 2004; Six et al., 2006). The Gram (+)/Gram (-) ratio decreased in zone 3 (≥ 15 m) in relation to the increase in SOM, total C and N content. Gram (-) bacteria are thought to be copiotrophic organisms with a high growth rate, using labile substrate such as in zone 3, while Gram (+) bacteria are thought to be oligotrophic organisms that are better decomposers of less

labile soil organic matter but have a lower growth rate (Fierer et al., 2007). Furthermore, the greater relative abundance of cyclopropanes close to the river (64% more than distal areas), which indicates the growth rate in the bacterial community and has been linked to changes in nutrient availability, infers that the most rapid growth or turnover rates will occur in distal areas of the river as a result of higher nutrient availability and lower stress conditions (i.e. water fluctuation) (Ponder and Tadros, 2002; Bossio et al., 2006).

4.2. N cycling across the riparian transect

The balance between the different steps of the N cycle varied along the riparian transect, while the plant and soil retention potential was constant, showing the varying potential of riparian wetland for N attenuation. The amount of N added did not exceed N plant demand, however, the total higher plant recovery of ^{15}N (ca. 30-40%) indicated a relatively high rate of removal. A similar amount of N was retained in the moss layer or soil (either in solution, sorbed to the solid phase, or immobilized in the microbial biomass) indicating that approximately 30-65% was lost by denitrification (as NO, N_2O or N_2), mass water flow, or translocated by roots out of the ^{15}N addition area. Our results are consistent with short-term ^{15}N recovery by vegetation in other non-riparian studies (e.g. grasslands; Nordbakken et al., 2003; Wilkinson et al., 2015). However, the high variability in ^{15}N recovery between replicates, most likely due to inherent heterogeneity in riparian areas, made it difficult to identify any consistent spatial patterns in N uptake across the riparian transect (Williams et al., 2015). Additionally, only short-term fate of urea-N was studied and differences in mass flow under the vegetation (and therefore ^{15}N residence time) was not accounted for (Weaver et al., 2001).

514 The genes abundance of the different steps of the N cycle showed niche
515 differentiation along the riparian transect. The *nifH* gene spatial distribution showed a
516 strong link to areas with lower soil water content, bulk density and higher porosity and
517 NH_4^+ concentrations, indicating the potential role of N fixation in zones 2 and 3 to
518 accumulate NH_4^+ in soil. This is consistent with these plant communities (e.g. *Calluna-*
519 *Eriophorum* and *Sphagnum* species) being severely N limited (Leppanen et al., 2015).
520 In contrast, AOA abundance followed the opposite trend than *nifH* gene, with the same
521 factors explaining their distribution. Thus, we conclude that nitrogen fixation and
522 nitrification are not coupled in the riparian wetland. This also implies that the archaea
523 are the main microorganisms involved in nitrification over bacteria (Caffrey et al., 2007;
524 Erguder et al., 2009). Thus, despite AOA and AOB delivering the same function, the
525 two communities live in distinct niches with different drivers. The low abundance of
526 AOB is likely due to the low soil pH (4.05 – 4.90), that favour AOA (Leininger et al.,
527 2006), while the drop in AOA abundance in distal zone could be related to the higher
528 concentration of NH_4^+ (Verhamme et al., 2011) or the change in soil water content.
529 Thus, the variation in ammonia oxidisers along the riparian transect will directly
530 affect the rate of denitrification. The constant NO_3^- concentration along the transect,
531 indicate that denitrification is occurring close to the river, which was confirmed by the
532 potential denitrification rates, highly stimulated by C addition (glucose), and to a lesser
533 extent by N (urea) in this area. It is well established that denitrification rates are usually
534 enhanced by anoxic conditions, high NO_3^- availability and labile organic C (Weier et al.,
535 1993). This is supported by the oligotrophic nature of the habitat, the high C-to-N ratio
536 of the soil, and the recalcitrant nature of the plant litter produced by the vegetation (Witt
537 and Setala, 2010). Although the *Calluna* heath soil possessed high levels of DOC, this
538 has previously been shown to be largely resistant to microbial attack due to its high

aromatic content (Stutter et al., 2013). Interestingly, N_2O production was stimulated greatly in the *Juncus effusus* zone when labile C was added, however, there was not a cumulative effect after the addition of C and N together. The low concentrations of NO_3^- in this zone also suggests that any NO_3^- produced could be lost to the river or is absorbed by plants. Overall, nitrification appears to be the rate limiting step in N cycling within the riparian wetland studied here.

With respect to the functional genes of the denitrifier community, none of the genes studied showed high abundance close to the river. Only the *nirS* gene displayed a higher abundance within zone 2, related to the increase in soil pH by less than a pH unit, highlighting the sensitivity of *nirS* gene abundance to pH (Liu et al., 2010). However, the relatively higher abundance of *nirS* was not translated into higher N_2O, although it should be noted that *nirS* and *nirK* code for nitrite reductase. The fungi, could also play a role in the denitrification as they possess *nirK* and *nirS* genes, which were not captured by the primers used. Some studies have indicated that N_2O emissions from fungal communities can be significant as they lack the *nosZ* gene to reduce N_2O to N_2; their contribution in riparian areas remains uncertain and further work is needed to explore their role further (Ma et al., 2008; Seo and DeLaune, 2010).

It is difficult to conclude on the potential N_2O emissions because the acetylene assay used in the study block the reduction of N_2O into N_2. The higher N_2O emissions close to the river after C and N addition could then be reduced. However, the constant *nosZ* clade I gene abundance and the absence of *nosZ* clade II gene along the transect, might indicate that N_2O is more likely to be emitted from the area close to the river, while the distal zone might be a sink for N_2O. Therefore, from a management perspective, restricted access to grazing and OM amendments which are commonly used for wetland restoration to accelerate soil development and regulate soil moisture

564 fluctuation, would be recommended to avoid future potential greenhouse gas emissions
565 in wetlands under grazing regimes (Bruland et al., 2009).
566 .

567 **5. Conclusions**

568 In terms of preventing freshwater pollution, riparian areas represent one of the
569 most valuable management tools for preventing excess nutrient loss from land to water.
570 Most studies to date, however, have focused on N and P cycling and transformations in
571 riparian soils adjacent to arable and intensively managed grasslands. Given the
572 heterogeneous nature of land use in many catchments, and the trend towards modelling
573 ecosystem services at the catchment scale, we need to gain a better understanding of
574 riparian N transformations across a variety of habitats and under different land use
575 intensities. Our study in an extensively managed agricultural system clearly showed that
576 changes in environmental factors such as breaks in vegetation or soil water saturation
577 provide strong indicators of the relative importance of different biotic and abiotic
578 processes involved in N cycling. However, our results also revealed hidden gradients in
579 microbial community structure and N cycling gene abundance across the riparian strip.
580 This reflects differences in key soil properties (e.g. organic matter content, redox) and
581 also possibly the source of nutrients flowing through the soil (i.e. in hyporheic water
582 flow versus lateral flow from upslope areas) and N_2O fluxes. This type of spatial
583 information can be used for more accurate mapping of ecosystem services at the
584 catchment scale and the design of better livestock management systems (e.g. prevention
585 of grazing in riparian areas to avoid N_2O emissions). While we have provided novel
586 insights into the dominant pathways for N removal in riparian zones, further work is
587 required to investigate if seasonal patterns exist and how closely gene abundance is
588 related to gene expression.

589

590 **Acknowledgements**

591 This research was supported by the UK Natural Environment Research Council under
592 the Macronutrients Programme from a NERC grant: NE/J011967/1: The Multi-Scale
593 Response of Water Quality, Biodiversity and Carbon Sequestration to Coupled
594 Macronutrient Cycling from Source to Sea. This research was also supported by a
595 Knowledge Economy Skills Scholarship (KESS 2) awarded to LDS funded via the
596 European Social Fund (ESF) through the European Union's Convergence program
597 administered by the Welsh Government.

598

599 **References**

600 Aulakh, M.S., Doran, J.W., Mosier, A.R., 1991. Field-evaluation of 4 methods for
601 measuring denitrification. Soil Science Society of America Journal 55, 1332-1338.
602 Avrahami, S., Bohannan, B. J., 2009. N_2O emission rates in a California meadow soil
603 are influenced by fertilizer level, soil moisture and the community structure of
604 ammonia-oxidizing bacteria. Global Change Biology 15, 643-655.
605 Bakken, L.R., Bergaust, L., Liu, B., Frostegård, Å., 2012. Regulation of denitrification
606 at the cellular level: a clue to the understanding of N_2O emissions from
607 soils. Philosophical Transactions of the Royal Society B 367, 1226-1234.
608 Balasooriya, W. K., Denef, K., Peters, J., Verhoest, N. E. C., Boeckx, P., 2007.
609 Vegetation composition and soil microbial community structural changes along a
610 wetland hydrological gradient. Hydrology and Earth System Sciences Discussions
611 4, 3869-3907.

612 Blossfeld, S., Gansert, D., Thiele, B., Kuhn, A.J., Losch, R., 2011. The dynamics of
613 oxygen concentration, pH value, and organic acids in the rhizosphere of *Juncus*
614 spp. Soil Biology & Biochemistry 43, 1186-1197.
615 Bohrer, K. E., Friese, C. F., Amon, J. P., 2004. Seasonal dynamics of arbuscular
616 mycorrhizal fungi in differing wetland habitats. Mycorrhiza 14, 329-337.
617 Bossio, D. A., Fleck, J. A., Scow, K. M., Fujii, R., 2006. Alteration of soil microbial
618 communities and water quality in restored wetlands. Soil Biology & Biochemistry
619 38, 1223-1233.
620 Bruland, G. L., Richardson, C. J., Daniels, W. L., 2009. Microbial and geochemical
621 responses to organic matter amendments in a created wetland. Wetlands 29, 1153-
622 1165.
623 Bundy, L.G., Meisinger, J.J., 1994. Nitrogen availability indices. p. 951-984. In R.W.
624 Weaver et al. (ed.). Methods of soil analysis. Part 2. SSSA Book series 5. Soil
625 Science Society of America, Madison, WI.
626 Burt, T. P., Matchett, L.S., Goulding, K.W.T., Webster, C.P., Haycock, N.E., 1999.
627 Denitrification in riparian buffer zones: the role of floodplain
628 hydrology. Hydrological Processes 13, 1451-1463.
629 Butterbach-Bahl, K., Baggs, E.M., Dannenmann, M., Kiese, R., Zechmeister-
630 Boltenstern, S., 2013. Nitrous oxide emissions from soils: how well do we
631 understand the processes and their controls? Philosophical Transactions of the
632 Royal Society B 368, 20130122.
633 Buyer, J.S., Sasser, M., 2012. High throughput phospholipid fatty acid analysis of soils.
634 Soil Biology & Biochemistry 61, 127-130.

635 Caffrey, J. M., Bano, N., Kalanetra, K., Hollibaugh, J. T., 2007. Ammonia oxidation
636 and ammonia-oxidizing bacteria and archaea from estuaries with differing histories
637 of hypoxia. ISME Journal 1, 660-662.
638 Canfield, D.E., Glazer, A.N., Falkowski, P.G., 2010. The evolution and future of
639 Earth's nitrogen cycle. Science 330, 192-196.
640 Chon, K., Chang, J.S., Lee, E., Lee, J., Ryu, J., Cho, J., 2011. Abundance of denitrifying
641 genes coding for nitrate (narG), nitrite (nirS), and nitrous oxide (nosZ) reductases in
642 estuarine versus wastewater effluent-fed constructed wetlands. Ecological
643 Engineering 37, 64-69.
644 De Sosa, L., Glanville, H.C., Marshall, M.R., Abood, S.A., Williams, A.P., Jones, D.L.,
645 2017. Delineating and mapping riparian areas for ecosystem service assessment.
646 Ecohydrology *in press*.
647 Di, H. J., Cameron, K. C., Shen, J. P., Winefield, C. S., O'Callaghan, M., Bowatte, S.,
648 He, J. Z., 2010. Ammonia-oxidizing bacteria and archaea grow under contrasting
649 soil nitrogen conditions. FEMS Microbiology Ecology 72, 386-394.
650 Di, H.J., Cameron, K.C., Podolyan, A., Robinson, A., 2014. Effect of soil moisture
651 status and a nitrification inhibitor, dicyandiamide, on ammonia oxidizer and
652 denitrifier growth and nitrous oxide emissions in a grassland soil. Soil Biology &
653 Biochemistry 73, 59-68.
654 Emmett, B.A., Cooper, D., Smart, S., Jackson, B., Thomas, A., Cosby, B., Evans, C.,
655 Glanville, H., McDonald, J.E., Malham, S.K., Marshall, M., Jarvis, S., Rajko-
656 Nenow, P., Webb, G.P., Ward, S., Rowe, E., Jones, L., Vanbergen, A.J., Keith, A.,
657 Carter, H., Pereira, M.G., Hughes, S., Lebron, I., Wade, A., Jones, D.L., 2016.
658 Spatial patterns and environmental constraints on ecosystem services at a catchment
659 scale. Science of the Total Environment 572, 1586-1600

660 Erguder, T. H., Boon, N., Wittebolle, L., Marzorati, M., Verstraete, W., 2009.
661 Environmental factors shaping the ecological niches of ammonia-oxidizing archaea.
662 FEMS Microbiology Reviews 33, 855-869.
663 Erisman, J.W., Galloway, J.N., Seitzinger, S., Bleeker, A., Dise, N.B., Petrescu,
664 A.M.R., Leach, A.M., de Vries, W., 2013. Consequences of human modification of
665 the global nitrogen cycle. Philosophical Transactions of the Royal Society B 368,
666 20130116.
667 Fierer, N., Bradford, M., Jackson, R., 2007. Toward an ecological classification of soil
668 bacteria. Ecology 88, 1354-1364.
669 Findlay, R.H., 2004. Determination of microbial community structure using
670 phospholipids fatty acid profiles. Molecular Microbial Ecology Manual Volume:
671 4.08, 983-1004. Kluwer Academic Publishers, Netherlands.
672 Frostegård, Å., Bååth, E., Tunlio, A., 1993. Shifts in the structure of soil microbial
673 communities in limed forests as revealed by phospholipid fatty acid analysis. Soil
674 Biology & Biochemistry 25, 723–730.
675 Gerdol, R., Anfodillo, T., Gualmini, M., Cannone, N., Bragazza, L., Brancaleoni, L.,
676 2004. Biomass distribution of two subalpine dwarf-shrubs in relation to soil
677 moisture and nutrient content. Journal of Vegetation Science 15, 457-464.
678 Groffman, P.M., Butterbach-Bahl, K., Fulweiler, R.W., Gold, A.J., Morse, J.L., Stander,
679 E.K., Tague, C., Tonitto, C., Vidon, P., 2009. Challenges to incorporating spatially
680 and temporally explicit phenomena (hotspots and hot moments) in denitrification
681 models. Biogeochemistry 93, 49-77.
682 Groffman, P.M., Hanson, G.C., 1997. Wetland denitrification: influence of site quality
683 and relationships with wetland delineation protocols. Soil Science Society of
684 America Journal 61, 323-329.

685 Gruber, N., Galloway, J.N., 2008. An Earth-system perspective of the global nitrogen
686 cycle. Nature 451, 293-296.
687 Gunina, A., Kuzyakov, Y., 2015. Sugars in soil and sweets for microorganisms: Review
688 of origin, content, composition and fate. Soil Biology & Biochemistry 90, 87-100.
689 Gutknecht, J. L., Goodman, R. M., Balser, T. C., 2006. Linking soil process and
690 microbial ecology in freshwater wetland ecosystems. Plant and Soil 289, 17-34.
691 Her, J.J., Huang, J.S., 1995. Influences of carbon surface and C/N ratio on nitrate nitrite
692 denitrification and carbon breakthrough. Bioresource Technology 54, 45-51.
693 Herbert, R.A., 1999. Nitrogen cycling in coastal marine ecosystems. FEMS
694 Microbiology Reviews 23, 563-590.
695 Jacinthe, P.A., Vidon, P., 2017. Hydro-geomorphic controls of greenhouse gas fluxes in
696 riparian buffers of the White River watershed, IN (USA). Geoderma 301, 30-41.
697 Jones, D.L., Darrah, P.R., 1996. Re-sorption of organic compounds by roots of *Zea*
698 *mays* L. and its consequences in the rhizosphere. III. Characteristics of sugar influx
699 and efflux. Plant and Soil 178, 153-160.
700 Jones, D.L., Willett, V.B., 2006. Experimental evaluation of methods to quantify
701 dissolved organic nitrogen (DON) and dissolved organic carbon (DOC) in soil. Soil
702 Biology & Biochemistry 38, 991-999.
703 Leininger, S., Urich, T., Schloter, M., Schwark, L., Qi, J., Nicol, G.W., Prosser, J.I.,
704 Schuster, S.C., Schleper, C., 2006. Archaea predominate among ammonia-
705 oxidizing prokaryotes in soils. Nature 442, 806–809.
706 Leppanen, S., Rissanen, A., Tiirola, M., 2015. Nitrogen fixation in Sphagnum mosses is
707 affected by moss species and water table level. Plant and Soil 389, 185-196.

Liu, B., Mørkved, P. T., Frostegård, Å., Bakken, L. R., 2010. Denitrification gene pools, transcription and kinetics of NO, N_2O and N_2 production as affected by soil pH. FEMS Microbiology Ecology 72, 407-417.

Lou, Y.J., Pan, Y.W., Gao, C.Y., Jiang, M., Lu, X.G., Xu, Y.J., 2016. Response of plant height, species richness and aboveground biomass to flooding gradient along vegetation zones in floodplain wetlands, Northeast China. Plos One 11, e0153972.

Lucas, R., Medcalf, K., Brown, A., Bunting, P., Breyer, J., Clewley, D., Keyworth S., Blackmore, P., 2011. Updating the Phase 1 habitat map of Wales, UK, using satellite sensor data. ISPRS Journal of Photogrammetry and Remote Sensing 66, 81–102.

Ma, W. K., Farrell, R. E., Siciliano, S. D., 2008. Soil formate regulates the fungal nitrous oxide emission pathway. Applied and Environmental Microbiology 74, 6690-6696.

Manter, D.K., Vivanco, J.M., 2007. Use of the ITS primers, ITS1F and ITS4, to characterize fungal abundance and diversity in mixed-template samples by qPCR and length heterogeneity analysis. Journal of Microbiological Methods 71, 7–14.

Marsden, K.A., Jones, D.L., Chadwick, D.R., 2016. The urine patch diffusional area: An important N_2O source? Soil Biology & Biochemistry 92, 161-170.

Matheson, F.E., Nguyen, M.L., Cooper, A.B., Burt, T.P., Bull, D.C., 2002. Fate of ^{15}N-nitrate in unplanted, planted and harvested riparian wetland soil microcosms. Ecological Engineering 19, 249-264.

Mayer, P. M., Reynolds, S. K., McCutchen, M. D., Canfield, T. J., 2007. Meta-analysis of nitrogen removal in riparian buffers. Journal of environmental quality 36, 1172-1180.

Miranda, K.M., Espey, M.G., Wink, D.A., 2001. A rapid, simple spectrophotometric method for simultaneous detection of nitrate and nitrite. Nitric Oxide Biology and Chemistry 5, 62-71.

Mulvaney, R.L., 1996. Nitrogen e inorganic forms. In: Sparks, D.L. (Ed.), Methods of Soil Analysis. Soil Science Society of America, American Society of Agronomy Inc., Madison, WI, pp. 1123-1184.

Murphy, J., Riley, J.P., 1962. A modified single solution method for the determination of phosphate in natural waters. Analytica Chimica Acta 27, 31-36.

Nijburg, J.W., Laanbroek, H.J., 1997. The influence of *Glyceria maxima* and nitrate input on the composition and nitrate metabolism of the dissimilatory nitrate-reducing bacterial community. FEMS Microbiology Ecology 22, 57-63.

Nordbakken, J.F., Ohlson, M., Högberg, P., 2003. Boreal bog plants: nitrogen sources and uptake of recently deposited nitrogen. Environmental Pollution 126, 191-200.

Ponder, F., Tadros, M., 2002. Phospholipid fatty acids in forest soil four years after organic matter removal and soil compaction. Applied Soil Ecology 19, 173-182.

Rydin, H., Jeglum, J.K., 2013. The Biology of Peatlands, 2nd Edition. Biology of Habitats Series, Oxford University Press, Oxford, UK.

Sanchez-Pérez, J.M., Iribar, A., Martinez, M., García-Linares, C., Antigüedad, I., 2003. Eliminación de nitratos por desnitrificación en la zona no saturada del suelo en un humedal del cinturón peri-urbano de Vitoria-Gasteiz, pp. 385-390. In: VI Jornadas sobre Investigación de la Zona no Saturada del Suelo, Valladolid, Spain.

Schnabel, R.R., Cornish, L.F., Stout, W.L., Shaffer, J.A., 1996. Denitrification in a grassed and a wooded, valley and ridge, riparian ecotone. Journal of Environmental Quality 25, 1230-1235.

Seitzinger, S., Harrison, J. A., Böhlke, J. K., Bouwman, A. F., Lowrance, R., Peterson, B., Drecht, G. V., 2006. Denitrification across landscapes and waterscapes: a synthesis. Ecological Applications 16, 2064-2090.

Selbie, D.R., Buckthought, L.E., Shepherd, M.A., 2015. The challenge of the urine patch for managing nitrogen in grazed pasture systems. Advances in Agronomy 129, 229-292.

Seo, D.C., DeLaune, R.D., 2010. Fungal and bacterial mediated denitrification in wetlands: influence of sediment redox condition. Water Research 44, 2441-2450.

Sharps, K., Masante, D., Thomas, A., Jackson, B., Redhead, J., May, L., Prosser, H., Cosby, B., Emmett, B., Jones, L., 2017. Comparing strengths and weaknesses of three ecosystem services modelling tools in a diverse UK river catchment. Science of the Total Environment 584, 118-130.

Six, J., Frey, S. D., Thiet, R. K., Batten, K. M., 2006. Bacterial and fungal contributions to carbon sequestration in agroecosystems. Soil Science Society of America Journal 70, 555-569.

Stutter, M.I., Richards, S., Dawson, J.J.C., 2013. Biodegradability of natural dissolved organic matter collected from a UK moorland stream. Water Research 47, 1169-1180.

Tabuchi, A., Kikui, S., Matsumoto, H., 2004. Differential effects of aluminium on osmotic potential and sugar accumulation in the root cells of Al-resistant and Al-sensitive wheat. Physiologia Plantarum 120, 106-112.

Tiedje, J.M., Simkins, S., Groffman, P.M., 1989. Perspectives on measurement of denitrification in the field including recommended protocols for acetylene based methods. Plant and Soil 115, 261-284.

780 Ullah, S., Faulkner, S.P., 2006. Denitrification potential of different land-use types in an
781 agricultural watershed, lower Mississippi valley. Ecological Engineering 28, 131-
782 140.
783 Veraart, A.J., de Bruijne, W.J., de Klein, J.J., Peeters, E.T., Scheffer, M., 2011. Effects
784 of aquatic vegetation type on denitrification. Biogeochemistry 104, 267-274.
785 Verhamme, D.T., Prosser, J.I., Nicol, G.W., 2011. Ammonia concentration determines
786 differential growth of ammonia-oxidising archaea and bacteria in soil microcosms.
787 The ISME Journal 5, 1067.
788 Visser, E.J.W., Bogemann, G.M., 2006. Aerenchyma formation in the wetland plant
789 *Juncus effusus* is independent of ethylene. New Phytologist 171, 305-314.
790 Vymazal, J., 2007. Removal of nutrients in various types of constructed
791 wetlands. Science of the Total Environment 380, 48-65.
792 Weaver, R.W., Lane, J.J., Johns, M.J., Lesikar, B.J., 2001. Uptake of ^{15}N by
793 macrophytes in subsurface-flow wetlands treating domestic
794 wastewater. Environmental Technology 22, 837-843.
795 Weier, K. L., Doran, J.W., Power, J.F., Walters, D.T., 1993. Denitrification and the
796 dinitrogen/nitrous oxide ratio as affected by soil water, available carbon, and
797 nitrate. Soil Science Society of America Journal 57, 66-72.
798 Wells, N.S., Baisden, W.T., Horton, T., Clough, T.J., 2016. Spatial and temporal
799 variations in nitrogen export from a New Zealand pastoral catchment revealed by
800 stream water nitrate isotopic composition. Water Resources Research 52, 2840-
801 2854.
802 Wheeler, B.D., 1999. Water and plants in freshwater wetlands. In: Hydroecology: Plants
803 and water in terrestrial and aquatic ecosystems, pp. 127-180, Eds. Baird, A., Wilby,
804 R.L., Routledge, London, UK.

Wierda, A., Fresco, L.F.M., Grootjans, A.P., van Diggelen, R., 1997. Numerical assessment of plant species as indicators of the groundwater regime. Journal of Vegetation Science 8, 707-716.

Wilkinson, A., Hill, P.W., Vaieretti, M.V., Farrar, J.F., Jones, D.L., Bardgett, R.D., 2015. Challenging the paradigm of nitrogen cycling: no evidence of in situ resource partitioning by coexisting plant species in grasslands of contrasting fertility. Ecology and Evolution 5, 275-287.

Williams, M.R., Buda, A.R., Elliott, H.A., Singha, K., Hamlett, J., 2015. Influence of riparian seepage zones on nitrate variability in two agricultural headwater streams. Journal of the American Water Resources Association 51, 883-897.

Witt, C., Setala, H., 2010. Do plant species of different resource qualities form dissimilar energy channels below-ground? Applied Soil Ecology 44, 270-278.

Xu, X., Ouyang, H., Richter, A., Wanek, W., Cao, G., Kuzyakov, Y., 2011. Spatio-temporal variations determine plant-microbe competition for inorganic nitrogen in an alpine meadow. Journal of Ecology 99, 563-571.

821 **Figure Legends**

822 **Fig. 1.** The Conwy catchment, North Wales, UK showing the location of the riparian
823 sampling area and the major land cover classes.

824 **Fig. 2**. Location of sample points across the riparian area. Different colours indicate
825 changes in vegetation. Zone 1 represents the area dominated by *Juncus effusus*,
826 Zone 2 corresponds to the transitional area between the grasses and the heath, and
827 Zone 3 represents the heathland with *Calluna vulgaris* and *Sphagnum* mosses as
828 the dominant species.

829 **Fig. 3.** Correlation bi-plot from the principal component analysis (PCA) on PLFA
830 microbial groups (%) with respect to distance from the river (n = 4). Zone 1
831 represents the area dominated by *Juncus effusus* and is closest to the river (2 and 5
832 m), zone 2 corresponds to the transitional area between the grasses and the heath
833 (10 m), and zone 3 represents the heathland with *Calluna vulgaris* and *Sphagnum*
834 mosses as the dominant species and the farthest points from the river (15 and 25
835 m). Correlation of PLFA microbial groups with the main axes are given by their
836 specific names and distance from the river by cluster centroids (average score on
837 each horizontal principal component (PC1) and vertical principal component
838 (PC2) with standards errors). Circles represents sample points within the same
839 zone.

840 **Fig. 4.** Total bacterial, archaeal and fungal gene copy numbers relative to distance from
841 the river. Same lower case letters indicate no significant differences (P > 0.05)
842 with respect to distance from the river according to one-way ANOVA and the
843 Tukey post-hoc test. Bars represent mean values (n = 4 for 10, 15 and 25 m, n = 3
844 for 2 m and n = 2 for 5 m) ± SEM. Distance from river corresponds to a change in
845 the vegetation as shown in Figure 2.

Fig. 5. Recovery of ^{15}N (% of total applied) from within the different fractions (shoots, roots, mosses and soil) represented by bars (n = 3 except moss in zone 1 where n = 1). Zone 1 represents the area dominated by *Juncus effusus* and is closest to the river (5 m), zone 2 corresponds to the transitional area between the grasses and the heath (10 m) and zone 3 represents the heathland with *Calluna vulgaris* and *Sphagnum* mosses as the dominant species and the farthest points from the river (25 m). Same lower case letters indicate no significant differences (P > 0.05) with respect to the different fractions within each zone according to one-way ANOVA and Tukey post-hoc test.

Fig. 6. Cumulative N_2O emissions via denitrification in unamended soil (control) or after the application of labile C (glucose) and N (urea) either alone or in combination. Same lower case letters indicate no significant differences (P > 0.05) with respect to distance from the river according to Welch's test and the Games-Howell post-hoc test. Same capital letters indicate no significant differences (P > 0.05) between treatments for each distance from the river according to one-way ANOVA and Tukey post-hoc test. Bars represent mean values (n = 4) ± SEM.

Fig. 7. Bacterial *amoA* (AOB), archaeal *amoA* (AOA), *nifH*, *nirS*, *nosK*, *nosZ* gene copy numbers relative to distance from the river. Same lower case letters indicate no significant differences (P > 0.05) relative to distance from the river according to one-way ANOVA and the Tukey post-hoc test. Bars represent mean values (n = 4 for 10, 15 and 25 m, n = 3 for 2 m and n = 2 for 5 m) ± SEM. Distance from river corresponds to a change in the vegetation as shown in Figure 2.

Spatial zoning of microbial function and plant-soil nitrogen dynamics across a riparian area

Laura L. de Sosa[a,*], Helen C. Glanville[a,b], Miles R. Marshall[c], A. Prysor Williams[a], Maïder Abadie[d], Ian M. Clark[d], Aimeric Blaud[d], Davey L. Jones[a]

[a] *School of Environment, Natural Resources & Geography, Bangor University, Deiniol Road, Bangor, Gwynedd, LL57 2UW, United Kingdom*

[b] *School of Geography, Geology and the Environment, Keele University, Keele, Staffordshire, ST5 5BG, United Kingdom*

[c] *Centre for Ecology and Hydrology, Environment Centre Wales, Deiniol Rd, Bangor, Gwynedd, LL57 2UW, United Kingdom*

[d] *Department of Sustainable Agriculture Sciences, Rothamsted Research, West Common, Harpenden, Hertfordshire, AL5 2JQ, United Kingdom*

* Corresponding author. School of Environment, Natural Resources & Geography, Bangor University, Deiniol Road, Bangor, Gwynedd, LL57 2UW, United Kingdom.

E-mail address: afs411@bangor.ac.uk (L.L. de Sosa).

Supplementary on-line information

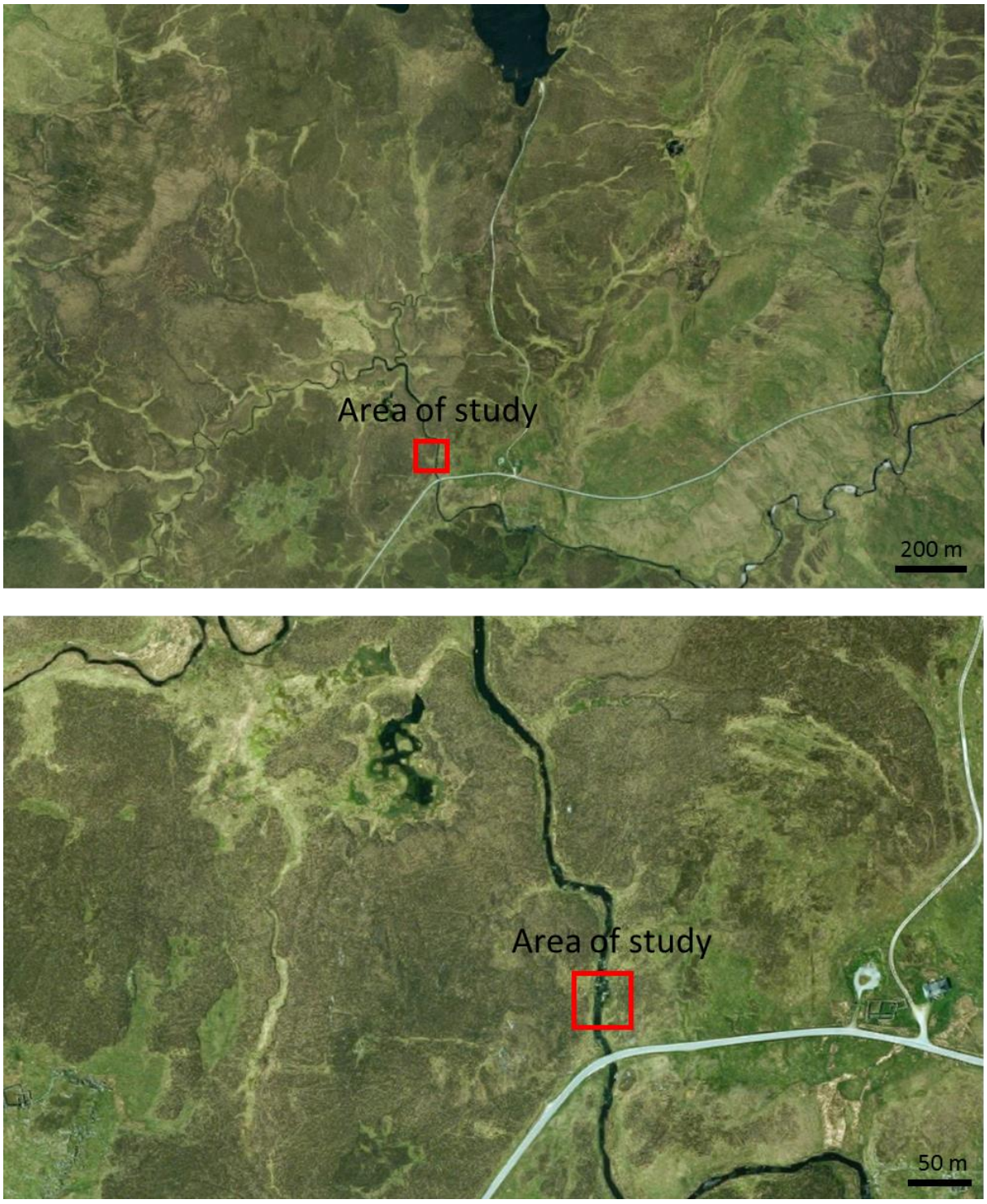

Fig. S1. Aerial photography of the area of study.

Fig. S2. Detailed photographs of vegetation in the area of study.

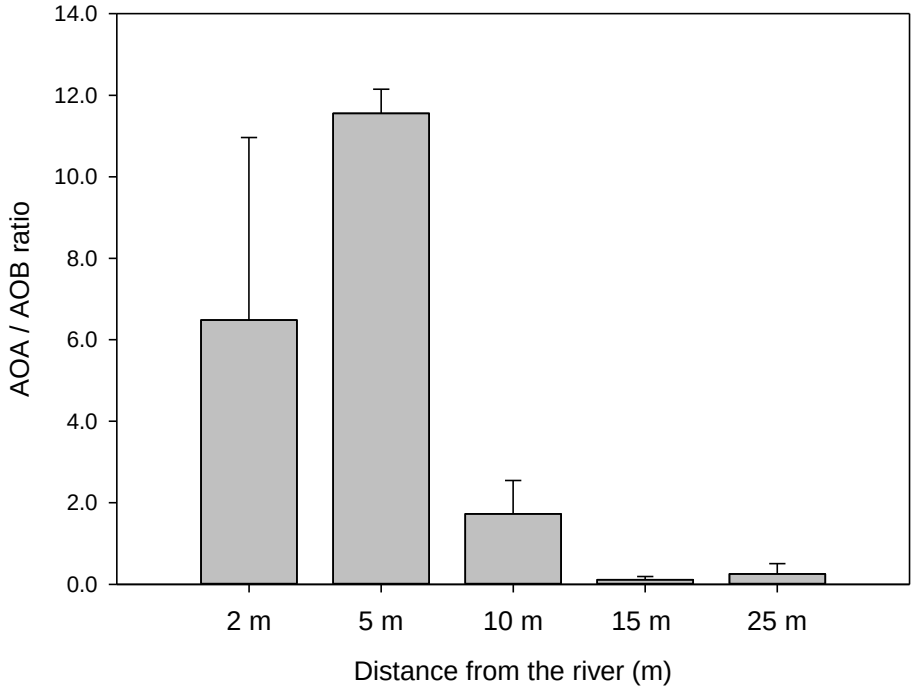

Fig. S3. Ratios of AOA to AOB *amoA* copy numbers relative to distance from the river. Bars represent mean values (n = 4 for 2, 10, 15 and 25 m and n = 2 for 5 m) ± SEM. Distance from river corresponds to a change in the vegetation as shown in Figure 3.

Table S1. PLFA biomarkers used for taxonomic microbial groups

Microbial group category	PLFA specific fatty acids			
AM Fungi	16:1 w5c			
Saprophytic Fungi	18:2 w6c			
Gram Negative	10:0 2OH	14:0 2OH	18:1 w6c	21:1 w8c
	10:0 3OH	16:1 w9c	18:0 cyclo w6c	21:1 w6c
	12:1 w8c	16:1 w7c	18:1 w3c	21:1 w5c
	12:1 w5c	16:1 w6c	19:1 w9c	21:1 w4c
	13:1 w5c	16:1 w4c	19:1 w8c	21:1 w3c
	13:1 w4c	16:1 w3c	18:1 w5c	22:1 w9c
	13:1 w3c	17:1 w9c	19:1 w6c	22:1 w8c
	12:0 2OH	17:1 w8c	19:0 cyclo w9c	22:1 w6c
	14:1 w9c	17:1 w7c	19:0 cyclo w7c	22:1 w5c
	14:1 w8c	17:1 w6c	9:1 w17c	22:1 w3c
	14:1 w7c	17:1 w5c	20:1 w9c	22:0 cyclo w6c
	14:1 w5c	17:1 w4c	20:1 w8c	24:1 w9c
	15:1 w9c	17:1 w3c	20:1 w6c	24:1 w7c
	15:1 w8c	16:0 2OH	19:0 cyclo w6c	11:0 iso 3OH
	15:1 w7c	17:0 cyclo w7c	20:1 w4c	14:0 iso 3OH
	15:1 w6c	18:1 w8c	20:0 cyclo w6c	
	15:1 w5c	18:1 w7c	21:1 w9c	
Methanotroph	16:1 w8c			
Eukaryote	15:4 w3c	19:3 w3c	22:5 w6c	23:3 w3c
	15:3 w3c	20:4 w6c	22:6 w3c	23:1 w5c
	16:4 w3c	20:5 w3c	22:4 w6c	23:1 w4c
	16:3 w6c	20:3 w6c	22:5 w3c	24:4 w6c
	18:3 w6c	20:2 w6c	22:2 w6c	24:3 w6c
	19:4 w6c	21:3 w6c	23:4 w6c	24:3 w3c
	19:3 w6c	21:3 w3c	23:3 w6c	24:1 w3c
Gram Positive	11:0 iso	14:0 iso	16:0 iso	17:1 anteiso w7c
	11:0 anteiso	14:0 anteiso	16:0 anteiso	19:0 iso
	12:0 iso	15:1 iso w9c	17:1 iso w9c	19:0 anteiso
	12:0 anteiso	15:1 iso w6c	17:0 iso	20:0 iso
	13:0 iso	15:1 anteiso w9c	17:0 anteiso	22:0 iso
	13:0 anteiso	15:0 iso	18:0 iso	
	14:1 iso w7c	15:0 anteiso	17:1 anteiso w9c	
Anaerobe	12:0 DMA	15:0 DMA	16:1 w5c DMA	18:1 w7c DMA
	13:0 DMA	16:2 DMA	16:0 DMA	18:1 w5c DMA
	14:1 w7c DMA	17:0 DMA	18:2 DMA	18:0 DMA
	14:0 DMA	16:1 w9c DMA	18:1 w9c DMA	
	15:0 iso DMA	16:1 w7c DMA		
Actinomycetes	16:0 10-methyl	18:1 w7c 10-methyl	22:0 10- methyl	
	17:1 w7c 10-methyl	18:0 10-methyl	20:0 10- methyl	
	17:0 10-methyl	19:1 w7c 10-methyl		

Table S2. List of the primers used to target each community.

Target gene	Primer	Sequence 5'-3'	References
Bacterial *16SrRNA*	341F	CCT AYG GGR BGC ASC AG	Glarling et al. (2015)
	806R	GGA CTA CNN GGG TAT CTA AT	
Archaeal *16SrRNA*	Parch519F	CAG CMG CCG CGG TAA	Øvreaset al. (1997)
	Arch1060R	GGC CAT GCA CCW CCT CTC	Reysenbach and Pace, (1995)
Fungal *ITS*	ITS1f	TCC GTA GGT GAA CCT GCG G	Gardes and Bruns (1993); Vilgalys and Hester (1990)
	5.8s	CGC TGC GTT CTT CAT CG	
nifH	PolF	TGC GAY CCS AAR GCB GAC TC	Poly et al. (2001)
	PolR	ATS GCC ATC ATY TCR CCG GA	
amoA Bacteria	amoA-1F	GGG GTT TCT ACT GGT GGT	Rotthauwe et al. (1997)
	amoA-2R	CCC CTC KGS AAA GCC TTC TTC	
amoA Archaea	Arch-amoAF	STA ATG GTC TGG CTT AGA CG	Francis et al. (2005)
	Arch-amoAR	GCG GCC ATC CAT CTG TAT GT	
nirK	nirK876F	ATY GGC GGV CAY GGC GA	Henry et al. (2004)
	nirK1040R	GCC TCG ATC AGR TTR TGG TT	
nirS	cd3aF	GTS AAC GTS AAG GAR ACS GG	Throbäck et al. (2004)
	R3cdR	GAS TTC GGR TGS GTC TTG A	
nosZ	nosZ1F	CGC RAC GGC AAS AAG GTS MSS GT	Henry et al. (2006)
	nosZ1R	CAK RTG CAK SGC RTG GCA GAA	
nosZII	nosZ-II-F	CTI GGI CCI YTK CAY AC	Jones et. al (2013)
	nosZ-II-R	GCI GAR CAR AAI TCB GTR C	

Table S3. Phospholipid fatty acid (PLFA) ratios of main microbial groups. Values represent means ± SEM (n = 4). Same lower case letters indicate no significant differences ($P > 0.05$) with respect to distance from the river according to one-way ANOVA and the Tukey post-hoc test.

PLFA ratio	Zone 1		Zone 2	Zone 3	
	2 m	5 m	10 m	15 m	25 m
Fungi/Bacteria	0.07 ± 0.01^{a}	0.07 ± 0.01^{a}	0.04 ± 0.004^{b}	0.03 ± 0.005^{b}	0.04 ± 0.006^{b}
Predator/Prey	0.03 ± 0.003^{a}	0.03 ± 0.001^{a}	0.02 ± 0.004^{a}	0.03 ± 0.004^{a}	0.03 ± 0.005^{a}
Gram +/Gram -	0.76 ± 0.03^{ab}	0.83 ± 0.04^{b}	0.88 ± 0.10^{b}	0.56 ± 0.01^{c}	0.61 ± 0.03^{ac}
Saturated/Unsaturated	1.01 ± 0.09^{a}	1.05 ± 0.10^{a}	1.38 ± 0.26^{a}	0.74 ± 0.04^{a}	0.88 ± 0.18^{a}
Mono/Poly	13.5 ± 1.18^{a}	14.4 ± 2.68^{a}	15.9 ± 1.76^{a}	17.6 ± 1.50^{a}	16.6 ± 2.44^{a}
16w/16 cyclo	3.31 ± 0.19^{a}	3.89 ± 0.23^{a}	4.11 ± 0.53^{a}	9.65 ± 0.54^{b}	9.20 ± 0.69^{b}
18w/19 cyclo	$0.70 \quad 0.07^{a}$	$0.64 \quad 0.04^{a}$	$0.85 \quad 0.11^{a}$	$1.93 \quad 0.08^{b}$	$2.06 \quad 0.25^{b}$

References

Francis, C.A., Roberts, K.J., Beman, J.M., Santoro, A.E., Oakley, B.B., 2005. Ubiquity and diversity of ammonia-oxidizing archaea in water columns and sediments of the ocean. Proceedings of the National Academy of Sciences of the United States of America 102, 14683–14688.

Gardes, M., Bruns, T.D., 1993. ITS primers with enhanced specificity for basidiomycetes - application to the identification of mycorrhizae and rusts. Molecular Ecology 2, 113–118.

Glaring, M.A., Vester, J.K., Lylloff, J.E., Al-Soud, W.A., Sørensen, S.J., Stougaard, P., 2015. Microbial diversity in a permanently cold and alkaline environment in Greenland. PLOS One 10, e0124863.

Henry, S., Baudoin, E., López-Gutiérrez, J.C., Martin-Laurent, F., Brauman, A., Philippot, L., 2004. Quantification of denitrifying bacteria in soils by *nirK* gene targeted real-time PCR. Journal of Microbiological Methods 59, 327–335.

Henry, S., Bru, D., Stres, B., Hallet, S., Philippot, L., 2006. Quantitative detection of the nosZ Gene, encoding nitrous oxide reductase, and comparison of the abundances of 16S rRNA, *narG*, *nirK*, and *nosZ* genes in soils. Applied and Environmental Microbiology 72, 5181–5189.

Jones, C.M., Graf, D.R.H., Bru, D., Philippot, L., Hallin, S., 2013. The unaccounted yet abundant nitrous oxide-reducing microbial community: a potential nitrous oxide sink. The ISME Journal 7, 417–426.

Øvreas, L., Forney, L., Daae, F.L., Torsvik, V., 1997. Distribution of bacterioplankton in meromictic Lake Saelenvannet, as determined by denaturing gradient gel electrophoresis of PCR-amplified gene fragments coding for 16S rRNA. Applied and Environmental Microbiology 63, 3367–3373.

Poly, F., Jocteur Monrozier, L., Bally, R., 2001. Improvement in the RFLP procedure for studying the diversity of nifH genes in communities of nitrogen fixers in soil. Research in Microbiology 152, 95–103.

Reysenbach, A.-L., Pace, N.R., 1995. Reliable amplification of hyperthermophilic archaeal 16S rRNA genes by the polymerase chain reaction, in: In Archaea: A Laboratory Manual. CSHL Press, New York, USA, pp. 101–105.

Rotthauwe, J.H., Witzel, K.P., Liesack, W., 1997. The ammonia monooxygenase structural gene *amoA* as a functional marker: molecular fine-scale analysis of natural ammonia-oxidizing populations. Applied and Environmental Microbiology 63, 4704–4712.

Throbäck, I.N., Enwall, K., Jarvis, Å., Hallin, S., 2004. Reassessing PCR primers targeting *nirS, nirK* and *nosZ* genes for community surveys of denitrifying bacteria with DGGE. FEMS Microbiology Ecology 49, 401–417.

Vilgalys, R., Hester, M., 1990. Rapid genetic identification and mapping of enzymatically amplified ribosomal DNA from several *Cryptococcus* species. Journal of Bacteriology 172, 4238–4246.

Table 1. Soil physicochemical properties across the riparian transect. Different zones indicate changes in vegetation community with zone 1 being closest to the river. Values represent means ± SEM (n = 4). Same lower-case letters indicate no significant differences (P > 0.05) with regard to distance from river according to One-way ANOVA and Tukey or Games-Howell post-hoc test. Results are expressed on a soil dry weight basis.

Soil property	Zone 1		Zone 2	Zone 3	
	2 m	5 m	10 m	15 m	25 m
pH	4.18 ± 0.08^{a}	4.24 ± 0.05^{a}	4.90 ± 0.09^{b}	4.12 ± 0.02^{a}	4.05 ± 0.01^{a}
EC (µS cm^{-1})	23.4 ± 3.2^{a}	21.1 ± 2.0^{a}	11.6 ± 1.0^{b}	23.3 ± 2.4^{a}	26.3 ± 1.8^{a}
Bulk density (g cm^{-3})	0.31 ± 0.019^{a}	0.20 ± 0.026^{a}	0.09 ± 0.005^{b}	0.09 ± 0.004^{b}	0.09 ± 0.008^{b}
Total porosity (cm^{3} cm^{-3})	0.78 ± 1.33^{a}	0.86 ± 1.88^{ab}	0.94 ± 0.36^{b}	0.94 ± 0.32^{b}	0.93 ± 0.54^{b}
Soil gravimetric water content (g kg^{-1} soil)	659 ± 28^{a}	720 ± 5^{a}	793 ± 34^{a}	892 ± 2^{b}	899 ± 0.6^{b}
Organic matter (g kg^{-1} soil)	364 ± 20^{a}	470 ± 12^{b}	542 ± 87^{ab}	953 ± 5^{c}	965 ± 4^{c}
NH_4^+-N (mg kg^{-1} soil)	5.06 ± 0.95^{a}	4.75 ± 0.70^{a}	9.50 ± 1.56^{ab}	18.5 ± 1.94^{b}	16.7 ± 3.43^{b}
NO_3-N (mg kg^{-1} soil)	9.38 ± 0.92^{a}	12.6 ± 2.40^{a}	8.12 ± 3.09^{a}	10.5 ± 1.95^{a}	8.00 ± 0.91^{a}
Available P (mg kg^{-1} soil)	5.82 ± 3.60^{a}	3.10 ± 1.11^{a}	5.99 ± 3.68^{a}	56.0 ± 10.1^{b}	50.5 ± 13.7^{b}
Total C (g kg^{-1} soil)	215 ± 9^{a}	281 ± 8^{b}	330 ± 57^{abc}	576 ± 4^{c}	588 ± 17^{c}
Total N (g kg^{-1} soil)	8.58 ± 0.61^{a}	12.0 ± 0.57^{b}	$15.5 \pm {}^{2.58^{ab}}_{c}$	17.1 ± 0.11^{c}	15.7 ± 0.38^{c}
C-to-N ratio	25.3 ± 0.77^{a}	23.5 ± 0.92^{ab}	21.3 ± 0.53^{b}	33.8 ± 0.32^{c}	37.0 ± 1.96^{c}
Dissolved organic C (g kg^{-1} soil)	0.24 ± 0.02^{a}	0.36 ± 0.02^{bc}	0.38 ± 0.07^{ab}	1.31 ± 0.18^{cd}	1.09 ± 0.14^{cd}
Total dissolved N (g kg^{-1} soil)	0.04 ± 0.005^{a}	0.05 ± 0.005^{a}	0.06 ± 0.009^{a}	0.44 ± 0.29^{a}	0.11 ± 0.025^{a}
Microbial biomass PLFA (mmol kg^{-1} soil)	1.12 ± 0.21^{a}	2.02 ± 0.27^{a}	3.83 ± 1.25^{ab}	7.58 ± 0.54^{b}	7.29 ± 1.70^{b}
AMOC (mg C-CO_2 kg^{-1} soil h^{-1})	0.23 ± 0.04^{a}	0.41 ± 0.06^{ab}	0.61 ± 0.16^{ab}	0.92 ± 0.14^{b}	0.98 ± 0.20^{b}
AMN (mg kg^{-1} soil)	69.0 ± 12.2^{a}	116 ± 13.7^{a}	104 ± 15.2^{a}	96.0 ± 8.27^{a}	97.8 ± 30.0^{a}

Electrical conductivity (EC). Phospholipid Fatty Acid Analysis (PLFA). Anaerobically mineralization organic carbon (AMOC). Anaerobically mineralization nitrogen (AMN).

Table 2. Spearman's rank correlation coefficients and *P*-values between soil physicochemical properties and abundance of functional genes (gene copies μg^{-1} DNA). Significant correlations are shown in bold.

Functional genes	Bacterial *16SrRNA*	Archaeal *16SrRNA*	Fungal *ITS*	*nifH*	Bacterial *amoA*	Archaeal *amoA*	*nirK*	*nirS*	*nosZ*
pH	**0.478**	0.131	0.071	-0.055	0.066	**0.614**	0.275	**0.515**	**0.495**
p-value	**0.033**	0.583	0.788	0.833	0.801	**0.009**	0.286	**0.034**	**0.043**
EC	**-0.450**	-0.128	-0.018	-0.151	-0.170	-0.471	**-0.522**	**-0.522**	**-0.627**
p-value	**0.047**	0.590	0.944	0.563	0.513	0.057	**0.031**	**0.031**	**0.007**
Bulk density	-0.040	**-0.568**	0.440	**-0.699**	0.419	**0.723**	-0.450	0.368	0.184
p-value	0.867	**0.009**	0.077	**0.002**	0.094	**0.001**	0.070	0.146	0.480
Total porosity	0.043	**0.562**	**-0.427**	**0.704**	-0.414	**-0.726**	0.454	-0.365	-0.168
p-value	0.856	**0.010**	**0.087**	**0.002**	0.098	**0.001**	0.067	0.150	0.519
Soil water content	-0.057	0.378	-0.249	**0.592**	-0.215	**-0.907**	0.215	-0.407	-0.316
p-value	0.810	0.101	0.335	**0.012**	0.408	**0.000**	0.408	0.105	0.216
Organic matter	-0.171	0.338	-0.218	**0.597**	-0.244	**-0.907**	0.261	-0.421	-0.360
p-value	0.471	0.144	0.400	**0.011**	0.345	**0.000**	0.311	0.093	0.155
NH_4^+-N	0.135	0.427	-0.108	**0.582**	-0.195	**-0.669**	0.297	-0.387	-0.333
p-value	0.571	0.060	0.680	**0.014**	0.453	**0.003**	0.247	0.125	0.191
NO_3-N	-0.236	-0.237	0.400	-0.173	-0.147	0.071	-0.387	-0.240	-0.184
p-value	0.317	0.314	0.112	0.507	0.573	0.786	0.124	0.352	0.480
Available P	0.103	**0.485**	-0.081	**0.457**	0.129	**-0.618**	0.116	-0.166	-0.218
p-value	0.665	**0.030**	0.757	**0.065**	0.622	**0.008**	0.656	0.525	0.400
Total C	-0.161	0.407	-0.294	**0.577**	-0.258	**-0.869**	0.253	-0.412	-0.440
p-value	0.497	0.075	0.252	**0.015**	0.318	**0.000**	0.328	0.100	0.077
Total N	-0.023	0.358	-0.007	**0.795**	-0.300	**-0.632**	**0.490**	-0.317	-0.105
p-value	0.925	0.121	0.978	**0.000**	0.241	**0.006**	**0.046**	0.216	0.687
Dissolved organic C	-0.029	0.343	-0.106	**0.580**	-0.201	**-0.674**	0.200	-0.361	-0.439
p-value	0.902	0.139	0.687	**0.015**	0.439	**0.003**	0.442	0.155	0.078
Total dissolved N	-0.062	0.236	0.058	**0.544**	-0.217	**-0.610**	0.201	-0.374	-0.341
p-value	0.796	0.317	0.826	**0.024**	0.403	**0.009**	0.439	0.139	0.181
Microbial biomass PLFA	-0.026	0.276	-0.044	**0.639**	-0.229	**-0.806**	0.256	-0.373	-0.203
p-value	0.912	0.238	0.866	**0.006**	0.376	**0.000**	0.321	0.140	0.434
AMOC	-0.229	-0.263	0.314	0.256	-0.294	-0.181	-0.009	-0.276	0.108
p-value	0.331	0.263	0.220	0.321	0.252	0.486	0.974	0.283	0.680
AMN	-0.033	0.057	0.171	**0.611**	-0.181	**-0.544**	0.316	-0.222	-0.049
p-value	0.890	0.810	0.513	**0.009**	0.486	**0.024**	0.216	0.392	0.852

Electrical conductivity (EC). Phospholipid Fatty Acid Analysis (PLFA). Anaerobically mineralizable organic carbon (AMOC).

Table 3. Spearman's rank correlation coefficients and *P*-values between soil physicochemical properties and N_2O emission (mg N kg^{-1} h^{-1}) in unamended soil (control) or after the addition of labile C and N.

Soil property	**N_2O emissions (Control)**	**N_2O emissions (C addition)**	**N_2O emissions (N addition)**	**N_2O emissions (C and N addition)**
Water content	0.24	-0.80	-0.71	-0.81
p-value	0.316	<0.001	<0.001	<0.001
Bulk density	-0.33	0.73	0.70	0.79
p-value	0.152	<0.001	0.001	<0.001
Total nitrogen	0.19	-0.89	-0.65	-0.74
p-value	0.431	<0.001	0.002	<0.001
Total porosity	0.33	-0.74	-0.69	-0.80
p-value	0.152	<0.001	0.001	<0.001
AMOC	0.31	-0.86	-0.70	0.82
p-value	0.179	<0.001	0.001	<0.001

Anaerobically mineralizable organic carbon (AMOC).

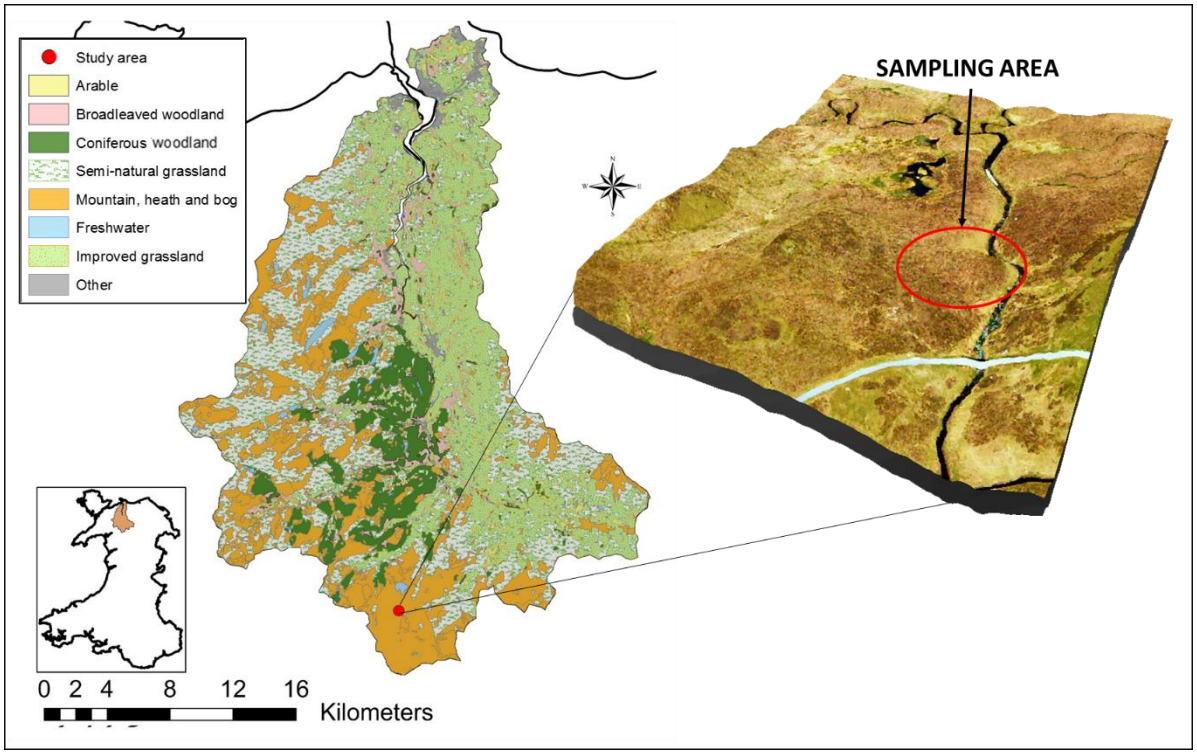

Fig. 1. The Conwy catchment, North Wales, UK showing the location of the riparian sampling area and the major land cover classes.

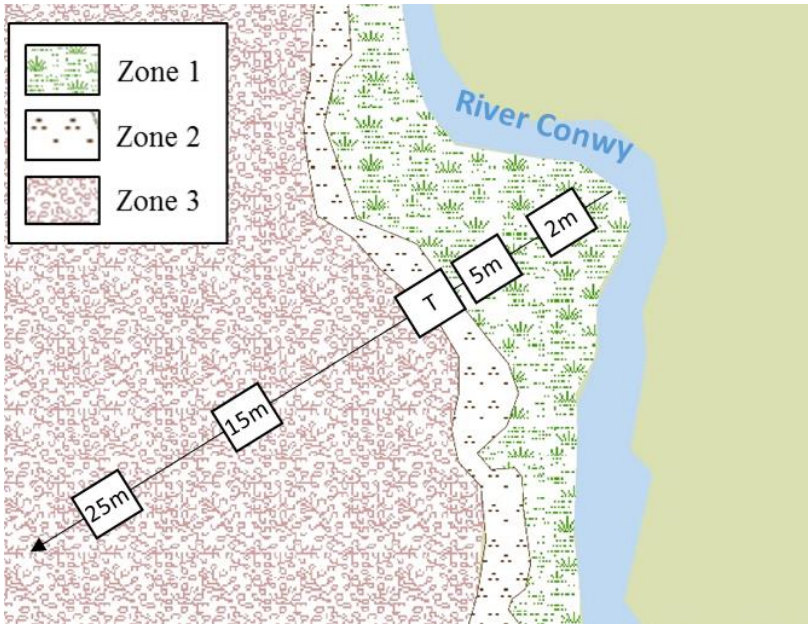

Fig. 2. Location of sample points across the riparian area. Different colours indicate changes in vegetation. Zone 1 represents the area dominated by *Juncus effusus*, Zone 2 corresponds to the transitional area between the grasses and the heath, and Zone 3 represents the heathland with *Calluna vulgaris* and *Sphagnum* mosses as the dominant species.

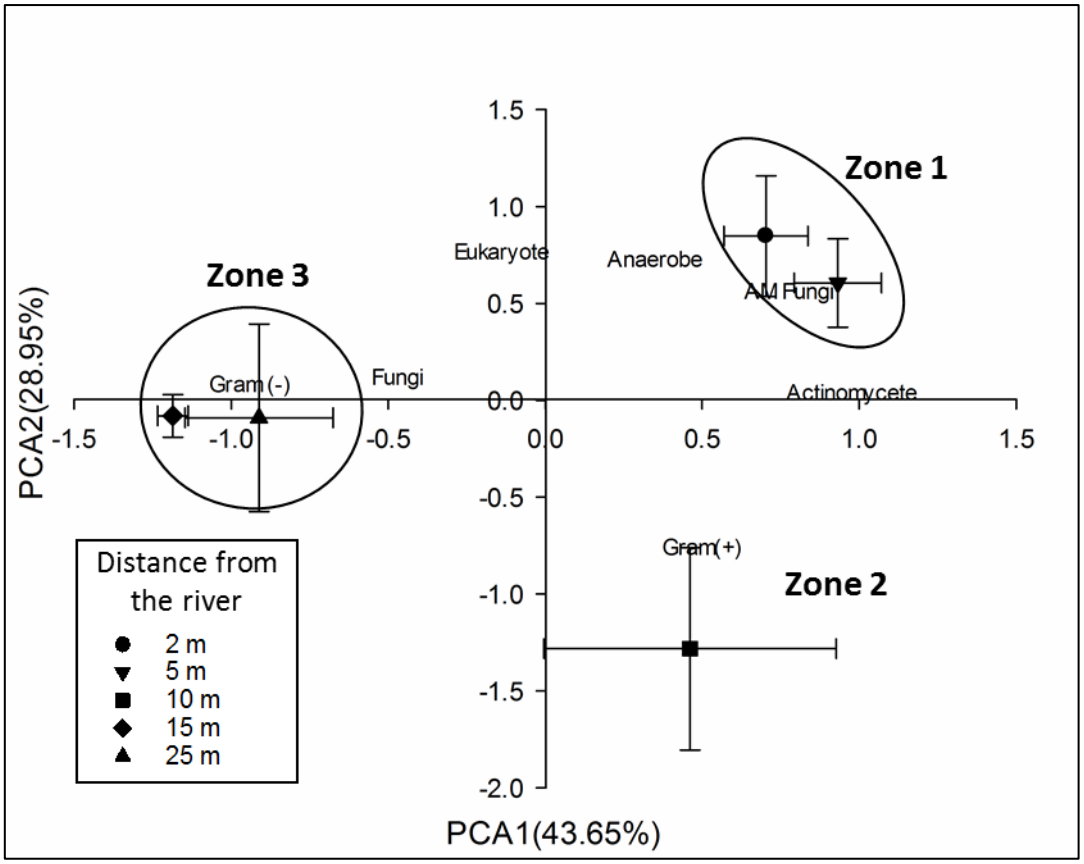

Fig. 3. Correlation bi-plot from the principal component analysis (PCA) on PLFA microbial groups (%) with respect to distance from the river (n = 4). Zone 1 represents the area dominated by *Juncus effusus* and is closest to the river (2 and 5 m), zone 2 corresponds to the transitional area between the grasses and the heath (10 m), and zone 3 represents the heathland with *Calluna vulgaris* and *Sphagnum* mosses as the dominant species and the farthest points from the river (15 and 25 m). Correlation of PLFA microbial groups with the main axes are given by their specific names and distance from the river by cluster centroids (average score on each horizontal principal component (PC1) and vertical principal component (PC2) with standards errors). Circles represents sample points within the same zone.

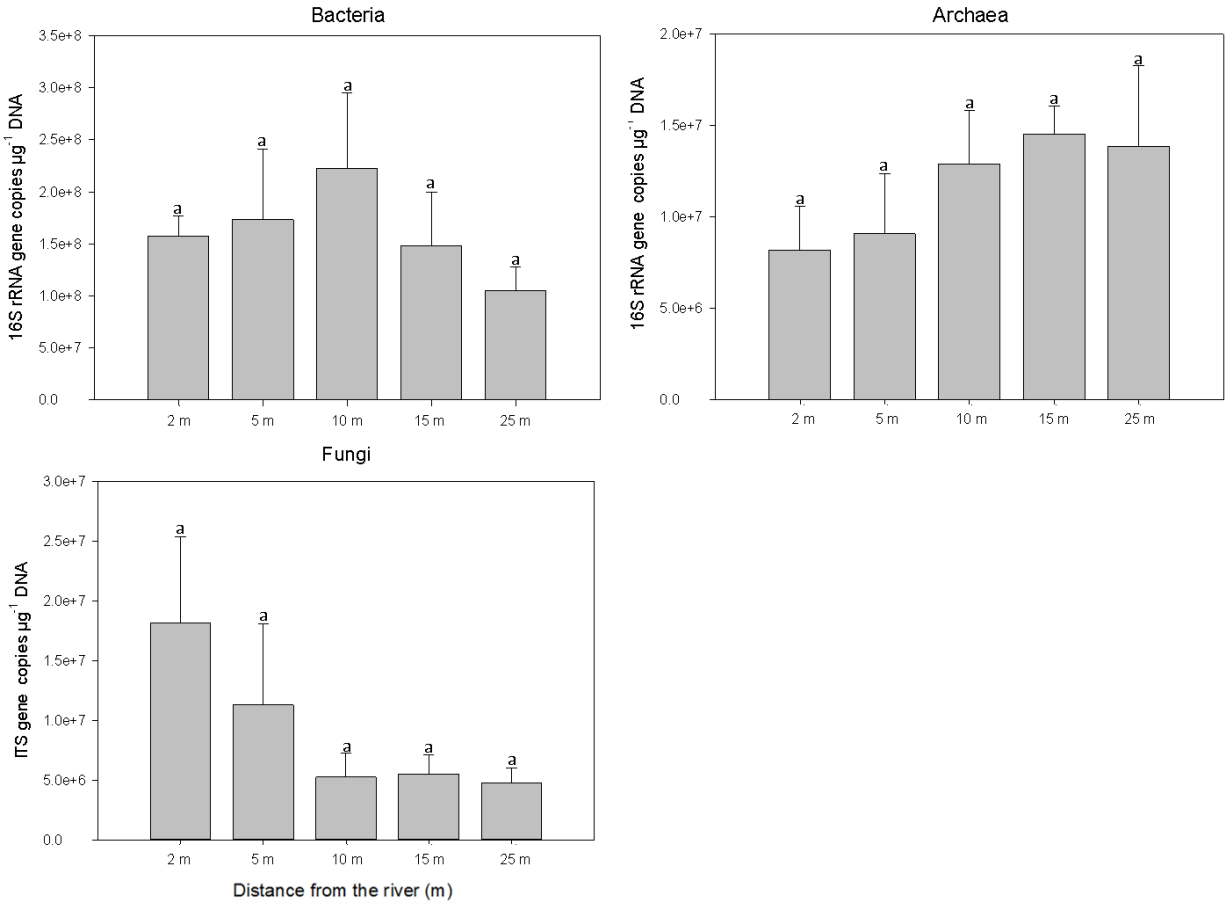

Fig. 4. Total bacterial, archaeal and fungal gene copy numbers relative to distance from the river. Same lower case letters indicate no significant differences ($P > 0.05$) with respect to distance from the river according to one-way ANOVA and the Tukey post-hoc test. Bars represent mean values ($n = 4$ for 10, 15 and 25 m, $n = 3$ for 2 m and $n = 2$ for 5 m) ± SEM. Distance from river corresponds to a change in the vegetation as shown in Figure 2.

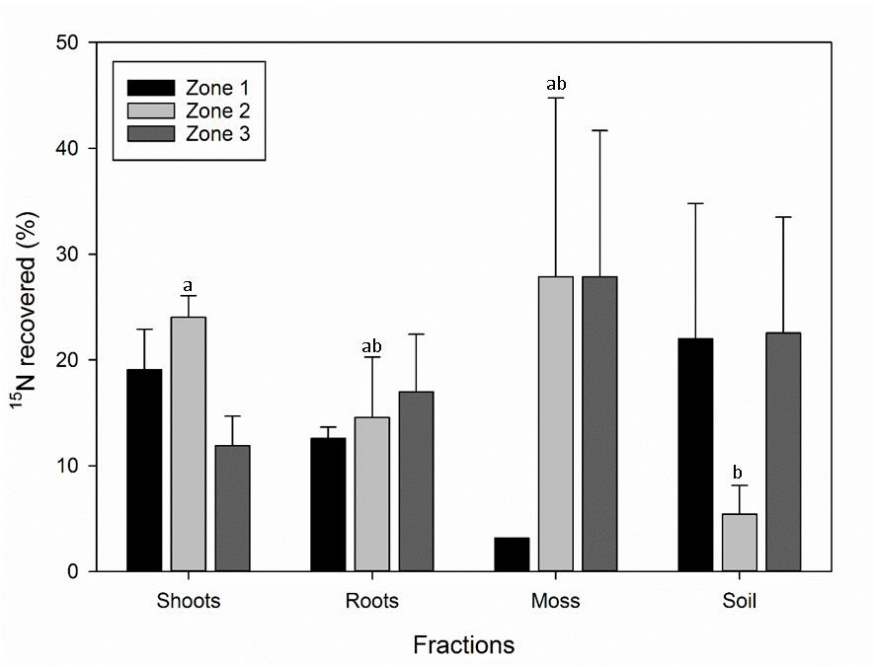

Fig. 5. Recovery of ^{15}N (% of total applied) from within the different fractions (shoots, roots, mosses and soil) represented by bars (n = 3 except moss in zone 1 where n = 1). Zone 1 represents the area dominated by *Juncus effusus* and is closest to the river (5 m), zone 2 corresponds to the transitional area between the grasses and the heath (10 m) and zone 3 represents the heathland with *Calluna vulgaris* and *Sphagnum* mosses as the dominant species and the farthest points from the river (25 m). Same lower case letters or the lack of it indicate no significant differences (P > 0.05) with respect to the different fractions within each zone according to one-way ANOVA and the Tukey post-hoc test.

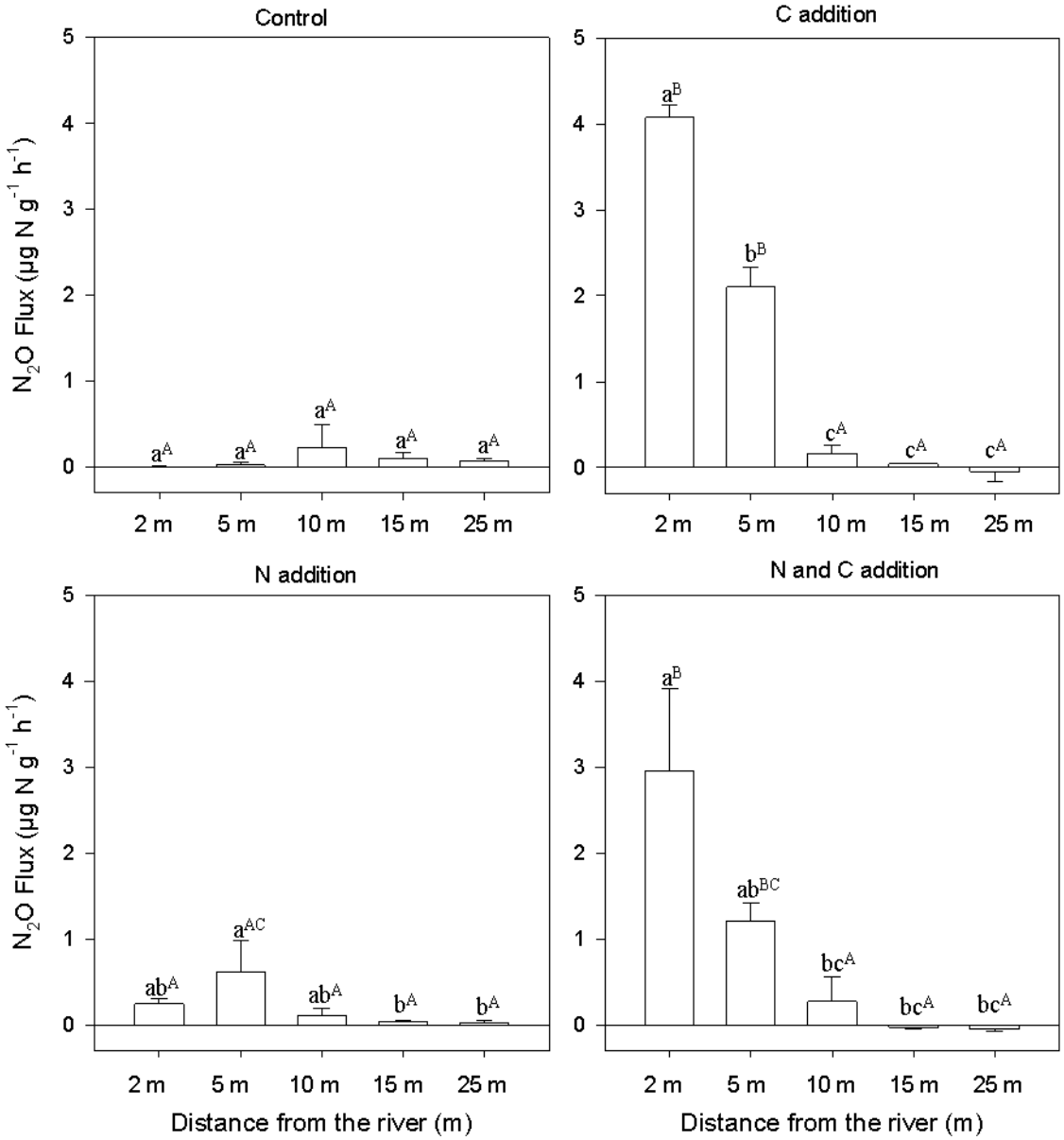

Fig. 6. Cumulative N_2O emissions via denitrification in unamended soil (control) or after the application of labile C (glucose) and N (urea) either alone or in combination. Same lower case letters indicate no significant differences ($P > 0.05$) with respect to distance from the river according to Welch's test and the Games-Howell post-hoc test. Same capital letters indicate no significant differences ($P > 0.05$) between treatments for each distance from the river according to one-way ANOVA and Tukey post-hoc test. Bars represent mean values ($n = 4$) ± SEM.

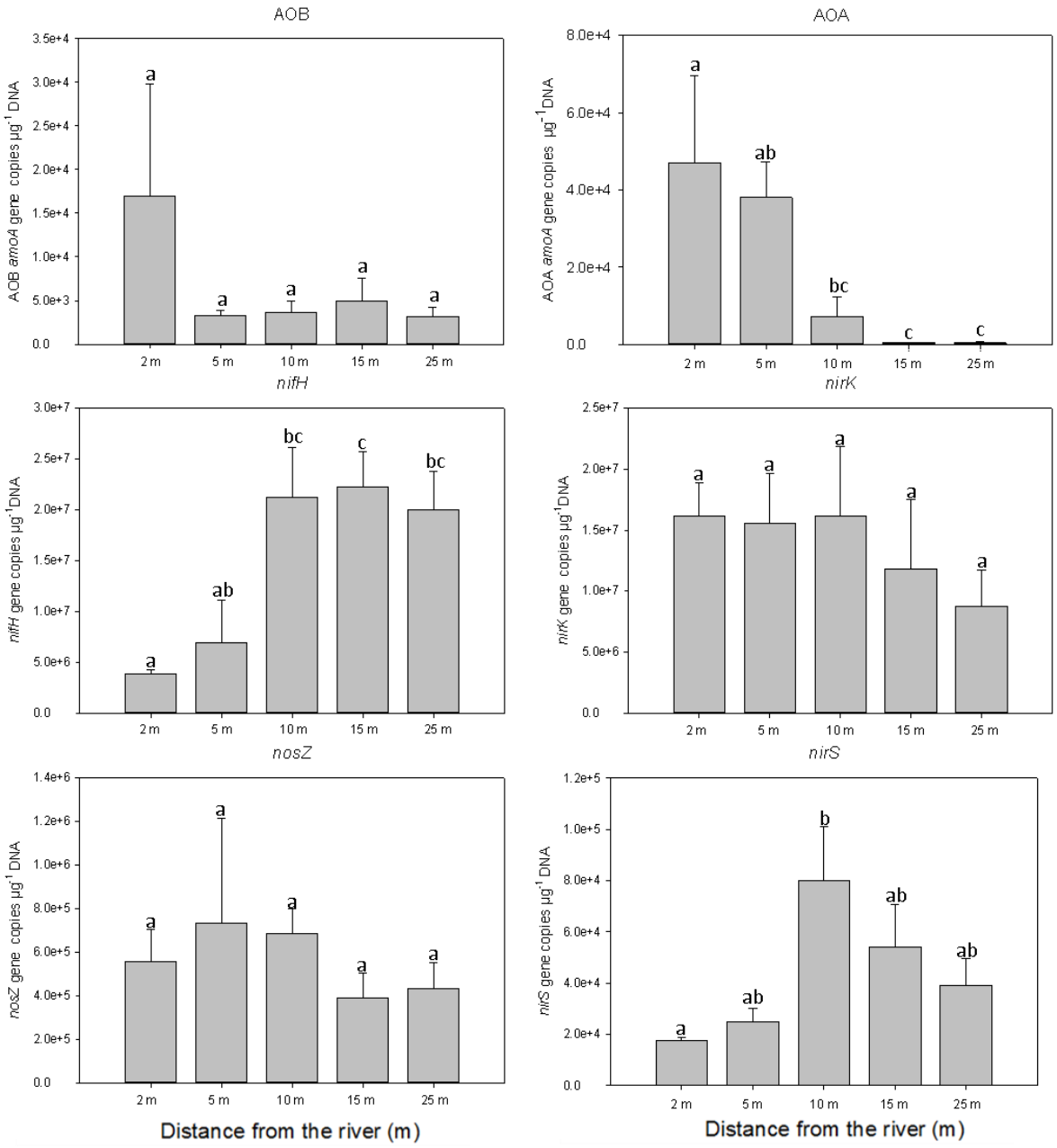

Fig. 7. Bacterial *amoA* (AOB), archaeal *amoA* (AOA), *nifH*, *nirS*, *nosK*, *nosZ* gene copy numbers relative to distance from the river. Same lower case letters indicate no significant differences ($P > 0.05$) relative to distance from the river according to one-way ANOVA and the Tukey post-hoc test. Bars represent mean values ($n = 4$ for 10, 15 and 25 m, $n = 3$ for 2 m and $n = 2$ for 5 m) ± SEM. Distance from river corresponds to a change in the vegetation as shown in Figure 2.

Research Highlights

- Microbial community structure changed with distance from the river.
- *amoA* gene abundance increased towards the river while *nifH* decreased.
- N_2O emissions rates were C limited but were greatest close to the river.
- Plant uptake of urea-^{15}N was high across the riparian zone.
- The spatial pattern of N removal by riparian plants and microbes was different.